HYDROLOGICAL RESPONSES TO LAND COVER CHANGES IN GILGEL ABBAY CATCHMENT, ETHIOPIA

Emiru Worku Kebede

March, 2009

HYDROLOGICAL RESPONSES TO LAND COVER CHANGES IN GILGEL ABBAY CATCHMENT, ETHIOPIA

by
Emiru Worku Kebede

Thesis submitted to the International Institute for Geo-information Science and Earth Observation in partial fulfilment of the requirements for the degree of Master of Science in Geo-information Science and Earth Observation, Specialisation: Integrated Watershed Modelling and Management

Thesis Assessment Board

Dr. Ir. M.W. Lubczynski	(Chairman)	WREM dept., ITC, Enschede
Dr. Ir. J. Schellekens	(External examiner)	Deltaris, Delft
Dr.Ing. T.H.M Rientjes	(First superviser)	WREM dept. ITC, Enschede
Dr. A.S.M Gieske	(Second superviser)	WREM dept. ITC, Enschede
Mr. Alemsegid Tamiru	(Advisor)	WREM dept. ITC, Enscede

INTERNATIONAL INSTITUTE FOR GEO-INFORMATION SCIENCE AND EARTH OBSERVATION
ENSCHEDE, THE NETHERLANDS

Disclaimer

This document describes work undertaken as part of a programme of study at the International Institute for Geo-information Science and Earth Observation. All views and opinions expressed therein remain the sole responsibility of the author, and do not necessarily represent those of the institute.

Dedicated to my mother Nigist Teferi, and my father Worku Kebede

Abstract

For the past 30 years an increase in population pressure caused a consistent change in the land cover of the Upper Gilgel Abbay catchment. This was mainly by deforestation as is the case in many other areas of Ethiopia as well The effects of land cover changes have impacted the water balance of the catchment by changing magnitude and pattern of runoff, peak flow and ground water levels. This study is mainly focusing on the assessment of the hydrological response due to the land cover change through satellite remote sensing and Geographic information system (GIS) integrated with the hydrologic modelling.

The result of remote sensing assessment on the land cover of the catchment indicated that the forest cover decreased by 1.38 % between the years 1973-1986, while it was 0.92 % between the years 1986-2001. This was mainly due to mainly the expansion of agriculture by 1.53 % and 1.07 % corresponding to the same period.

Based on this result, the stream flow records were analysed statistically to evaluate if changes in the land cover affected the hydrological response of the catchment. The result of the analysis indicated that the peak flow increased by 0.901 m^3/s and the base flow in the dry season also decreased by 0.053 m^3/s during the first period. For the record period the peak flow increased by 0.762 m^3/s while base flow decreased by 0.069 m^3/s. Generally, the analysis indicated that flow during the wet season has increased, while the flow during the dry season decreased. The HBV model was applied to evaluate the model response to the land cover changes, and the results show that the changes in stream flow characteristics could be relayed to the change of the land cover during the studied period.

Key words: Upper Gilgel Abbay, Land cover change, Remote sensing, GIS, Stream flow change; HBV

Acknowledgements

Above all Praise be to the Almighty, Gracious and Saviour God for his uncontested mercy and grace during my whole time I stayed in ITC.

First and for most I would like to gratefully acknowledge The Netherlands Government through the Netherlands Fellowship Programme (NFP) for granting me the opportunity to study at ITC.

I am deeply indebted to my supervisor Dr. Ing. T. H. M. Rientjes for his supervision, encouragement and guidance he has provided me throughout my research. His critical comments and helpful guidance give me a chance to explore further. I have learned a lot from him. I never forget your treatment, patience and devotion when my healthy was not good during the all research time. You are a special person with a great heart.

My deepest gratitude goes to my second supervisor Dr. Ambro Geiske. His kind support and encouragement gives me strength right from the inception of the topic to the last minute of the research.

I am very grateful to my Advisor Mr. Alemsegid Tamiru for all his support, encouragement, advice, the information he has given to me from the beginning of the topic and the knowledge he has shared me since the proposal writing, during the field work and afterwards. I learnt patience from you during the research work. His help is unforgettable.

I gratefully acknowledge to all offices and personalities who have given me data for my study, Ministry of water resources of Ethiopia and Ethiopian Meteorological Agency. I would like to extend my gratitude to Mr. Surafel (Hydrology department), for his kind advice and the data he and his office has provided me.

I am very grateful to my beloved wife Wehiba and my daughter Amen for their patience and encouragement while I feel tire you take long time to treat me.

I would like to extend my appreciation to my course mate for their support, socialization and help each other. Every body was wonderful in the cluster. I will not forget the Ethiopian fellow friends for their support and encouragement in times of pressure and stress.

Last but not least, I would like to thank my lecturers for giving me all the basics of science and their courage to help everybody. My thanks also goes to every staff in the program and the institute.

Table of contents

List of figures

List of tables

1. INTRODUCTION

1.1. Back ground

Land cover changes commonly are highly pronounced in the developing counties that are characterized by agriculture based economics and rapidly increasing human populations. Meyer and Turner (1994) discussed that land cover changes are caused by a number of natural and human driving forces. Whereas natural effects such as climate change are only over a long period of time, the effects of human activities are immediate and often direct. From the human factors, population growth is the most important in Ethiopia (Hurni, 1993 as cited in Tekele and Hedlund, 2000), as it is common in developing countries. Some 85% of the population of lives in rural areas and directly depend on the land for its livelihood. This means the demands of lands are increasing as population increases.

Population growth causes degradation of resources that relay on the available land and the interaction between them is very complex. Interactions can make positive or negative effects to the resources. People demand land for food production as well as for housing and it is common practice to clear the forest to make farming area and housing. The result is that land cover and land use change due to daily human intervention. Hence, understanding how the land cover change influence the river basin hydrology will enable planners to formulate policies to minimize the undesirable effects of future land cover changes.

Land cover changes may have immediate and long-lasting impacts on terrestrial hydrology which have been described by Calder (1993) and, alter the long term balance between rainfall and evapotranspiration and the resultant runoff. In the short-term, destructive land use change may effect the hydrological cycle either through increasing the water yield or through diminishing, or even eliminating the low flow in some circumstances (Croke et al., 2004). Savenije (1995) suggested that in the long-term the reductions in evapotranspiration and water recycling arising from land cover changes may initiate a feedback mechanism that results in reduced rainfall.

Study of stream flow patterns with respect to land cover dynamics enables assessment of sustainability of land use systems; because stream flows reflect on the hydrological state of the entire watershed. As stated by Calder (2002), the hydrological impact of land cover changes is a referencing issue and much research is necessary.

The information can also be applied to forecast the likely effects of any potential changes in land cover on water resource systems. Generally, it is appropriate to use satellite remote sensing and Geographic information system (GIS) integrated with the hydrological modelling to analyse the hydrological response due to the land cover change.

1.2. Problem statement

Gilgel Abbay catchment is densely populated with an annual growth rate of 2.31% according to CSA (central statistical authority) .This causes many effects on the resource bases such as deforestation, overgrazing of the range lands, and expansion of the residential area and agriculture area. Based on the field visit in September 2008, large deforestation is a day by day activity of the people living in the catchment. There is also high gully erosion by the effects of intense rainfall and topographic steepness of the catchment which aggravates the land cover change of the catchment. This continuous change in land cover has impacted the water balance of the catchment by changing the magnitude and pattern of runoff, the peak flow, ground water tables and thus the intermittence of once perennial steams or vice versa, which results increasing the extent of the water management problem. Therefore, a strong need is identified for the use of hydrologic techniques and tools that can assess the likely effects of land cover changes on the hydrologic response of a catchment. Such techniques and tools can provide information that can be used for sound water resources management at a catchment scale . In this study area, any change in stream flow patterns associated with land cover dynamics are poorly documented. Hence, such study has practical relevance for devising strategies and policies for a sustainable land and water use.

1.3. Objectives, research questions and hypothesis

The general objective of the study is to asses the hydrologic response due to the land cover changes in Gilgel Abbay catchment through remote sensing and hydrologic models.

1.3.1. General Objectives

The general objective of the study is to asses the hydrologic response due to the land cover changes in Gilgel Abbay catchment through remote sensing and hydrologic models.

1.3.2. Specific objectives

- To analyse hydrologic time series related to land cover change
- To quantify the land cover changes by change detection method.
- To evaluate the response of a hydrologic model of the catchment to the changes in land cover

To address the aforementioned objectives, the research questions for this study are:

- What trend in land cover change can be identified in the catchment?
- Have the land cover changes affected the rainfall runoff relation?
- How will the land cover changes affect the hydrologic response of the catchment?

1.3.3. Research hypothesis

- Catchments under little vegetation cover and hill slopes are subjected to high surface runoff volumes, low infiltration rate and reduced ground water recharge.

- The HBV model approach is able to simulate the hydrological response of the catchment in the study area.
- There is a significant variation of land cover changes between the referenced periods of the study (1975-2003) in the catchment.
- The hydrology behaviour of the catchment is highly affected by the land cover change.

1.4. General methodology

The methodology of the research has three phases:

Pre-field work

The main activities conducted before the field works were literature review on related works and previous studies including discussions with supervisors. Preparation the land cover maps of the study area using aster image of April, 2002 through unsupervised classification. Finally, collecting information about the study area and preparing a detailed action plan of field work that helps to adapt easily during the field visit.

Field work

The required hydrological and meteorological data from respective offices like daily discharge, daily rain fall, maximum and minimum temperature, sunshine hours and wind speed as well as 1:50,000 topographic map of the study area were collected during the field work. Moreover, during a survey of the catchment, ground truth data was collected using GPS for land cover classification and an interview was also conducted with local people to gather information about the land cover of the study area.

Post- field work

The main activities conducted after the field works were as follows: image classification and change detection techniques were analysed to identify land cover changes by processing the selected image data. The hydro-meteorological data was processed to analyse the results from data processing, and then converting the image and hydro-meteorological data processing to reflect and to match model parameters. Finally, the results of the modelling with respect to land cover changes were analysed.

Generally, the conceptual frame work in figure 1.1 shows the main procedure that was followed to investigate the hydrological response of land cover change.

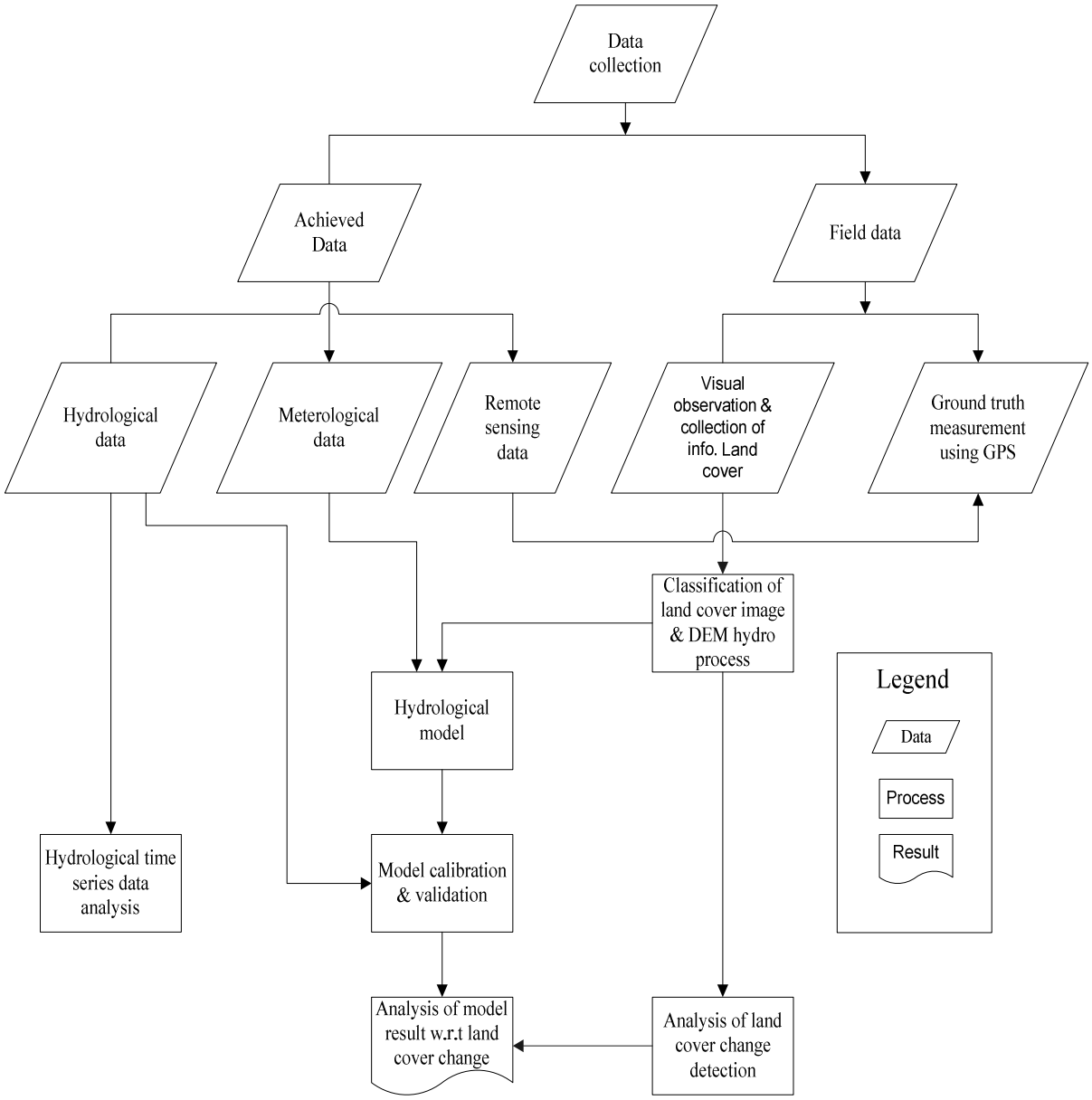

Figure 1-1: Frame work of the study

1.5. Thesis outline

This thesis report consists of six chapters. The contents of each chapter are organized as follows:

In the first chapter, a general introduction about land cover change and hydrological responses is presented. The problem statement, the research objectives and the research questions are also discussed in this chapter. The second chapter gives a brief introduction of the study area. The location, topography, climate and land cover of the study area are also described in this chapter. In the third chapter, literature review about the subject matter is presented and it gives a scientific review this study is mainly based on. The reviewed literatures are relevant to land cover classification,

change detection and hydrologic impact of land cover change. The fourth chapter is about the materials and methods used in this study. The fifth chapter presents the results and a discussion on the results of this study. The last chapter, six, gives the conclusions drawn from the study and the recommendations based on the study conducted to indicate direction for future studies.

2. STUDY AREA AND DATA AVAILABLITY

2.1. Study area

2.1.1. Location

Upper Gilgel Abbay catchment is located in the Northwest high lands of Ethiopia between 10^0 56' to11^0 22' N latitude and 36^0 44' to 37^0 03' E longitudes. The Upper Gilgel Abbay River is one of the major rivers which drains into Southern part of Lake Tana and originates from a small spring that is Gish Abbay Mountain near Sekela town at elevation of 2900 m a.m.s.l. At the outlet to Wotet Abbay, the catchment area is around 1656.20 km^2 with a longest flow path of the river from the source to the gauging station (Wotet Abbey) is 84 Km from SRTM.

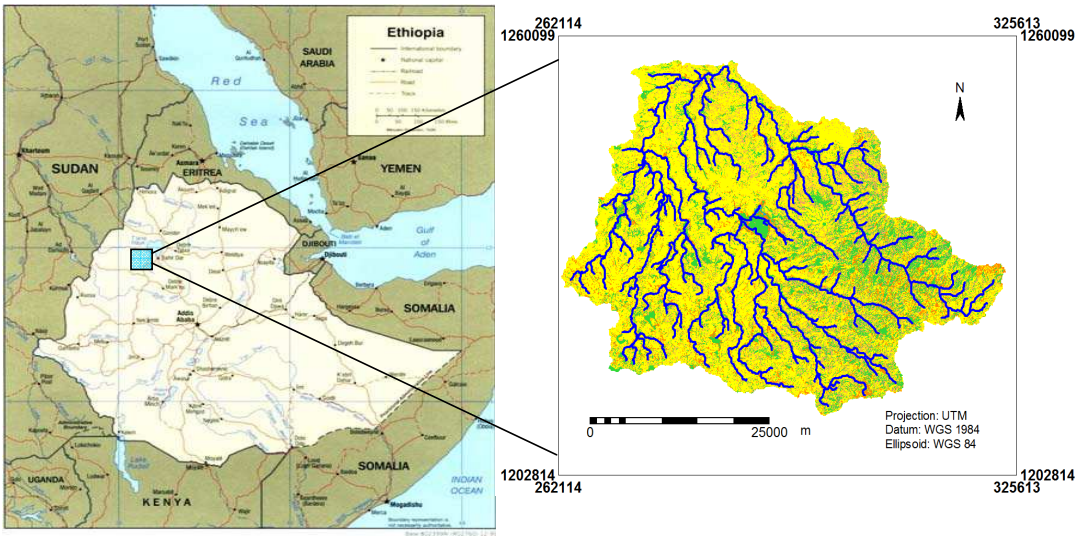

Figure 2-1: Location of Upper Gilgel Abbay Catchment

2.1.2. Topography

The elevation of Upper Gilgel Abbay catchment varies from 1934 to 2917 m a.m.s.l. by SRTM-DEM as shown in figure 2.2. On the South eastern ridges and Northern most parts of the catchments the highest elevation ranges and the lowest ranges are located respectively. The slope of the catchment was classified to gentle (0-6 %), steep (7-14%) and excessive (>14%) slope classes (Scottand and Hofer, 1995).

According to Ashenafi (2007) around 80 % of the catchment area falls in the slope range of (0-6 %), 15 % of the area falls in the slope range of (7-14 %) and the remaining 5 % is steeper than (14 %). It was also stated that the excessive slope of the catchment area lies in South east and decreases to the North.

Generally the catchment area is mountainous and is a highly dissected terrain with steep slopes in the upstream part, and an undulating topography and gentle slopes in the downstream part. This is Body text style. Use this for the body text.

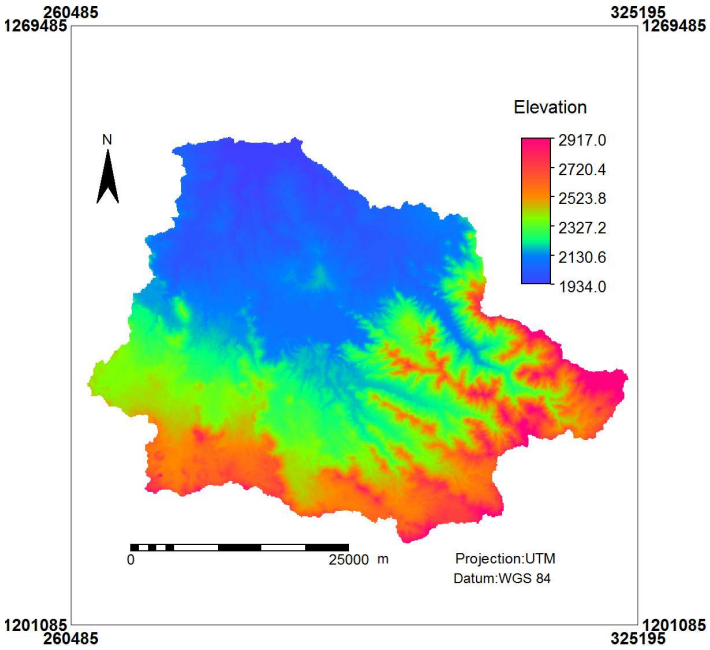

Figure 2-2: SRTM DEM of the Upper Gilgel Abbay catchment.

2.1.3. Climate

The inter-annual oscillation of the surface position of the ITCZ causes variations in the wind flow patterns in Ethiopia. In its oscillation to the north and south of the equator, the ITCZ passes over Ethiopia twice a year and this migration alternatively causes the onset and withdrawals of winds from north and south (EMA, 1981). The Upper Gilgel Abbay catchment receives big rains between June and September when the ITCZ is to the north of Ethiopia, while the small rainy season is usually between March and May. Winds from the gulf of Eden and Indian Ocean highs are drawn towards centre of Ethiopia. These moist easterly and south-westerly winds produce the small rains of spring to the east central part of the north-western highlands (Kahsay, 2004).

Generally, the annual climate of the study area may be classified in rain (June to September) and dry seasons (October to May). There is high spatial and temporal variation of rainfall in the study area. The spatial variation of rainfall amount in the area indicated a decreasing trend from south to north part of the catchment area. The long term mean annual rainfall in the southern part of the catchment (Sekela) and from the northern part to be of (Abbay Shelko) 1900 mm and 1200mm respectively.
Temperature in the study area is highly influenced by the altitude where the temperature decreases with increase in altitude. The mean annual temperature of the catchment falls in the range of 16^{o}C to 20^{o}C.The climate is generally temperate at higher elevations and tropical at the lower elevation (Conway, 1997).

2.1.4. Land cover

Rain fed agriculture is the main economic activity of the catchment. Irrigated land and perennial crops also cover large parts of the catchment. The land cover map of the Upper Gilgel Abbay catchment was prepared for this study by using supervised land cover classification of Landsat ETM image dated on 05 Feb. 2001. Most of the catchment area is dominated by agricultural land while limited areas in the south-east corner are covered by little vegetation. The major land cover types are shown in figure 4.3 and indicate that agricultural lands cover some 62 %, agriculture some 17 %, shrubs land some 9 %, grass land some 9 % and water and marshy lands some 3 %.

2.1.5. Soil and geology

The Upper Gilgel Abbay catchment is part of the highlands that largely owe their altitude to the uplift of the Arabo-Ethiopian landmass and the subsequent outpouring of basaltic lava flowing during the Tertiary period. This consists of Quaternary volcanic rocks that overlay the older Tertiary rocks of the catchment. The Quaternary Volcanics are mostly represented by olivine alkali basalt, often interbedded with clayey palaeosoils. As discussed in SMEC (2007) the Quaternary volcanic comprises blocky and fractured vesicular basalt, some basaltic breccias and tuffs perhaps as much as 200-300mm thick. The Upper Gilgel Abbay catchment is mostly covered by Haplic Luvisoils (BECOM, 1998). The FAO (1991) description states that the Luvisols are, in general, fertile soils because of their mixed mineralogy, relatively high mineral content and the presence of weatherable minerals. Generally, Tessema (2007) reported that the cultivated lands throughout the study area mostly lie on this type of soil.

2.2. Data availablity

2.2.1. Meteorological data

Based on the objective of the study, meteorological data are collected during the field campaign from the Ethiopian National Meteorological Agency (NMA) in Addis Ababa and BahirDar office. According to NMA, Meteorological data is categorized into four classes depending on the type of the data and its observation frequencies at each station. Based on this classification, meteorological stations found in this catchment are grouped into three classes. Dangila and Adet stations (class I with observation frequency of every three hours) have maximum and minimum temperature, wind speed, sunshine hour duration, relative humidity and precipitation. Kidimaja and Wotet Abbay stations (class III) have maximum and minimum temperature, and precipitation data where as Abbay shelko and Inijibara (class IV) stations have only observed daily precipitation data. In summary, the data has been collected from eight metrological stations within and around the catchment as shown in figure 2.3.

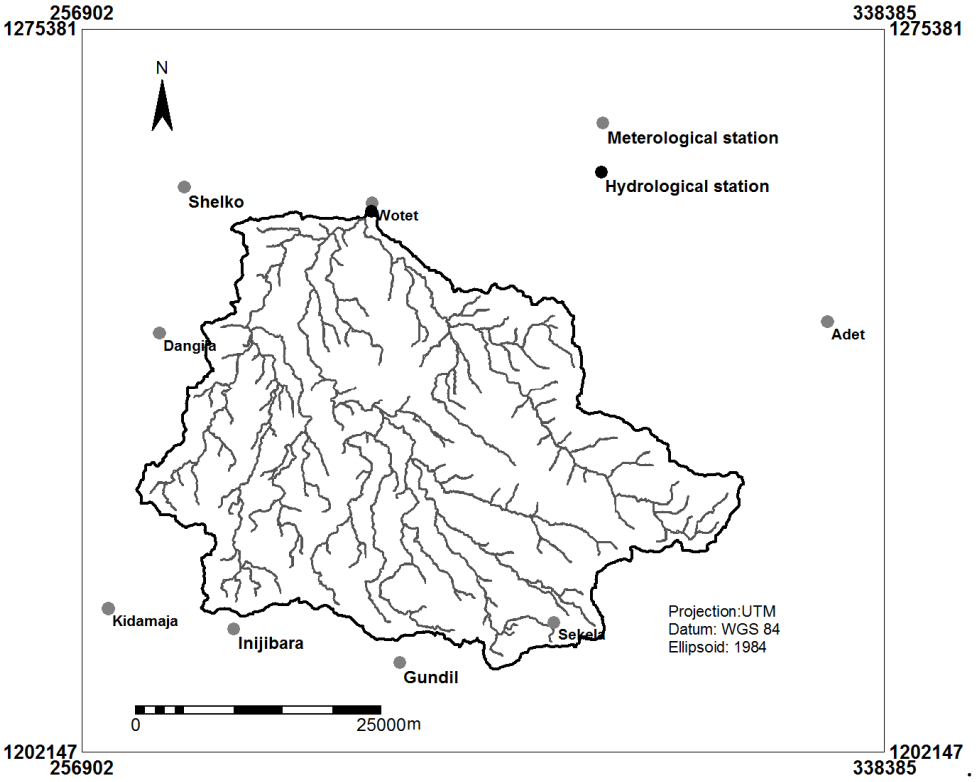

Figure 2-3: Meteorological and hydrological stations selected for the catchment.

Generally, daily rainfall data of 11 years have been collected from the period of 1987−1990 and 1999 −2005. For these years, temperature (max and min), sunshine hours, wind speed and relative humidity data have also been collected that were used for the calculation of evapotranspiration.

Table 2-1: Location of the meteorological stations

Stations name	Latitude (deg)	Longtiude (deg)
Adet	11.27	37.47
Dangila	11.12	36.83
Kidimaja	11	36.8
Inijibara	10.97	36.9
Wotet Abbay	11.37	37.05
Sekela	11	37.22
Gundil	10.95	37.07
Shelko	11.38	36.87

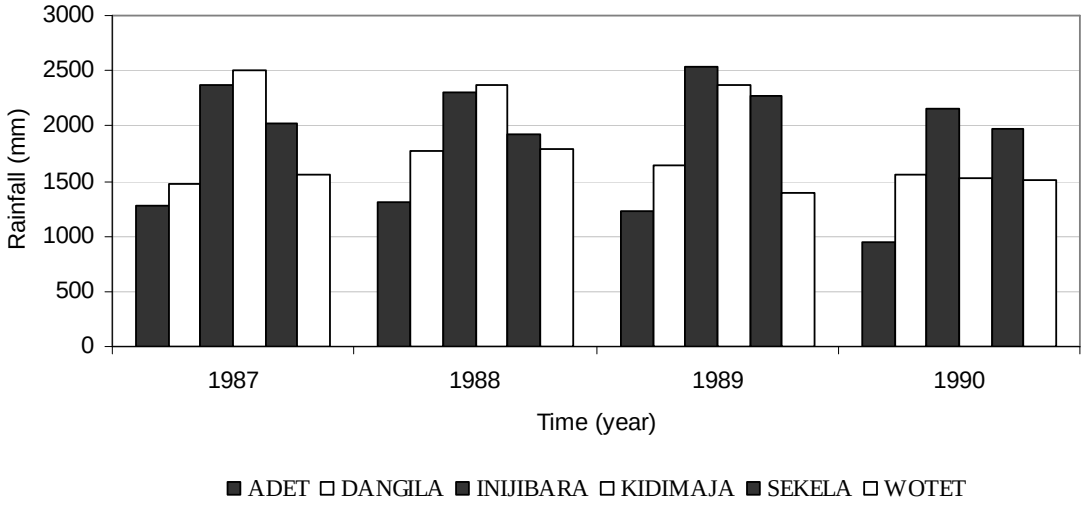

Figure 2-4: Annual rainfall of selected meteorological stations for the period of 1987-1990

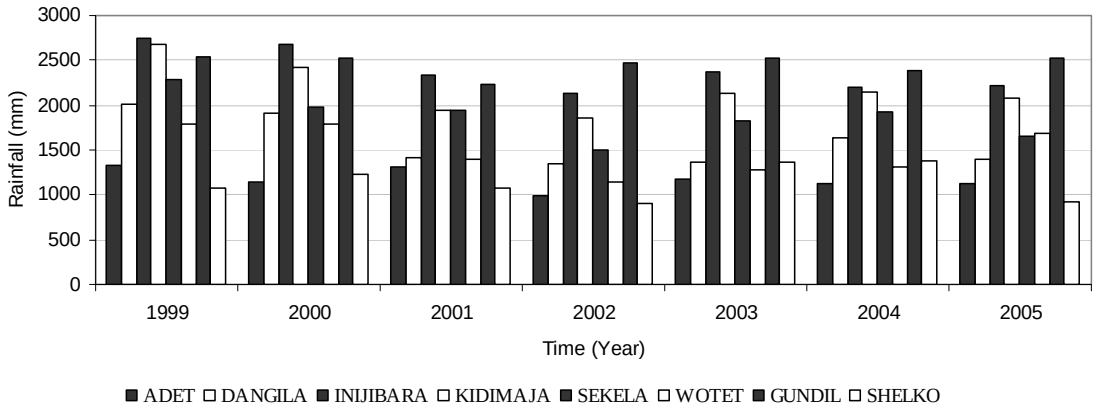

Figure 2-5: Annual rainfall of selected meteorological station for the period 1999-2005

2.2.2. Hydrological data

Daily series of discharge data of the upper Gilgel Abbay River were collected from the Ministry of Water Resources of Ethiopia (MOWR) during the field work. The river discharge of Gilgel Abbay is measured twice per day, one reading in the morning (6:00 hr) and one is in the afternoon (18:00 hr), at Wotet Abbay gauging station. The available discharge data is in the unit of m^3s^{-1}. The data covers a time period of 31 years which is from the period 1973 to 2003. The minimum discharge lies between 200 - 300 m^3/s, while the maximum discharges is between 300 – 500 m^3/s. A time series plot of the river discharge data is shown in figure 2.5. All discharge records of the year 1985 are considered since there is no indication of failure of the gauging station or differently.

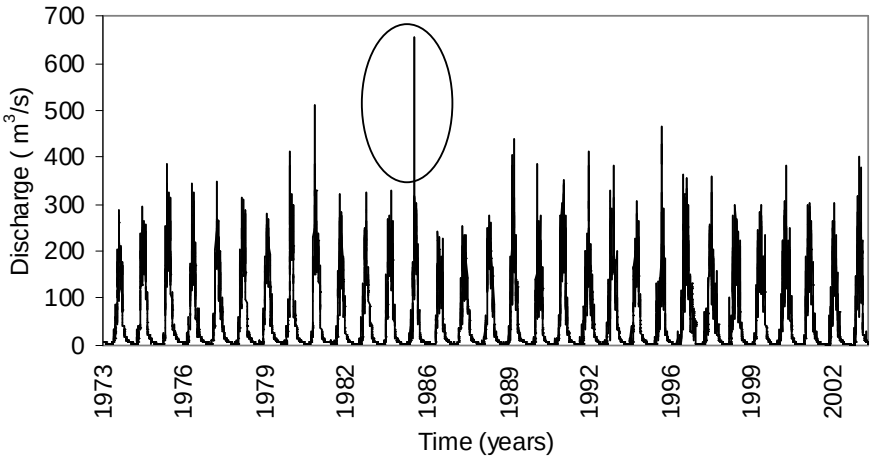

Figure 2-6: Discharge record of Gilgel Abbay River at Wotet Abbay station (1973-2003)

3. LITERATURE REVIEW

3.1. Land cover classfication

The purpose of digital land cover classification is to link the spectral characteristics of the image to a meaningful information class value, which can be displayed as a map so that resource managers or scientists can evaluate the landscape in an accurate and cost-effective manner (Weber and Dunno, 2001).The overall objective of image classification procedures is to automatically categorize all pixels in an image into land-cover classes. This may be achieved by either visual or computer aided analysis.

A large number of classification methods exist which are generally grouped in unsupervised and supervised classification. The classification may be either by an unsupervised method that groups cases by their relative spectral similarity or by a supervised method based on similarity of cases to a set of predefined classes that have been characterized spectrally.

Accuracy assessment is an important feature of land cover mapping that helps to determine the quality and reliability of information derived from remote sensed data. It also creates on continuity to understanding the thematic uncertainty, and its likely implication to end-users.

3.2. Land cover change detection

Land cover refers to the surface cover including geographical features like vegetation, urban infrastructure, water, barren land, inland water bodies, etc. Land cover is a fundamental variable that impacts on and links many parts of the human and physical environments. Barnsley (2001) refers to land cover as “the physical materials on the surface of a given parcel of land (e.g., grass, concrete, tarmac, water).” Land cover change is highly affected by human-induced activities rather than natural events. Today, mainly agriculture expansion, burning activities or fuel wood consumption, deforestation, expansion of grazing land, some construction works and urbanization cause land cover changes. Consequently, such changes may have great impacts on the catchment by altering hydrological processes such as infiltration, groundwater recharge, and base flow and run-off and assessing such is at the core of this work.

Change detection is the process of identifying differences in the state of a feature by observing it at different moments in time. There are a large number of change detection algorithms or techniques developed and used over the years to estimate changes using remote sensing data. These techniques are based on various mathematical and/or statistical relationships, principles, and assumptions (Singh, 1989). Change detection algorithms include image overlay, image digitizing, image differencing, image regression, image rationing, vegetation index differencing, principal component analysis, spectral/ temporal classification, post classification comparison, change vector analysis, and background subtraction (Singh, 1989; Coppin & Bauer, 1996; Sunar, 1998). Although these methods have been successfully applied in monitoring changes for several applications, there is no consensus

as to a 'best' change detection approach. The type of change detection method employed largely depends on data availability, the geographic area of study, time and computing constraints, and type of application.

Within the context of the change detection analyses, in this study, post classification comparison technique and matrix analysis have been used to determine the changes in land cover over 30 years. The advantage of post classification comparison is that it bypasses the difficulties associated with the analysis of the images acquired at different times of the year, or by different sensors and quite high change detection accuracy (Alphan, 2003). This is perhaps the most common approach to the change detection, and the methods comparison uses separate classifications of the images that occurred at different moment in time to produce different maps from which "from-to" change information can be generated (Jensen, 2004).

Matrix analysis produces a thematic layer that contains a separate class for every coincidence of classes in two layers. The output is best described with a matrix diagram. In this diagram, the classes of the two input layers represent the rows and columns of the matrix. The output classes are assigned according to the coincidence of any two input classes. If there is no change in the land cover over years, only values appear in the diagonal of the matrix, and these values represent the areas of the land classification. Under such circumstances, the sum of the columns and rows are similar and do not show any changes.

3.3. Remote sensing application

In most parts of the world, land cover is dynamic, especially in rural and semi rural areas. Under such condition, accurate, meaningful and availability of data on land is highly essential for planning and decision making. Among the various sources of land cover data, satellite remote sensing is particularly attractive. The importance of remote sensing was emphasized as a "unique View" of the spatial and temporal dynamics of the processes in land cover changes (Herold , 2003). Stefanov (2001) described that satellite remote sensing techniques have started to be used in 1970's as a modern tools to detect and monitor land cover change at various scales with useful results.

The change in land cover from rural to urban conditions and mapping of land cover establishes the baseline to predict to plan water resources, to monitor adjacent environmentally sensitive areas, and to evaluate development, resource management, industrial activity, and/or reclamation efforts. The vital component of mapping is to show the land cover changes in the watershed area and to divide land use in the various classes of land use. At this stage, remotely sensed imagery is of great help for obtaining information on temporal trends and spatial distribution of watershed areas and possible changes over the time dimension for projecting land cover changes but also to support changes impact assessment (Atasoy et al., 2006). Furthermore, multitemporal remotely sensed images are widely considered effective data sources that can be used to monitor the rapid changes of land cover, to classify types of land cover, and to obtain a timely regional overview of land cover information in a practical and economical manner over large areas.

In general, change evaluation in land cover can be obtained by using the analysis of multitemporal images to extract more classes or sub-classes besides the broad land cover types which used in the change detection limited by the historical map (Goetz *et al*., 1999; Prol-Ledesma *et al*., 2002). The acquisition of series of appropriate satellite images is often not possible for some change applications due to low spatial and spectral resolution.

In cases when large areas are to be analyzed for the study of times series historical land cover change, it is necessary to use LANDSAT Enhanced Thematic mapper (ETM+), LANDSAT Thematic Mapper (TM), as well as LANDSAT Multispectral Scanner (MSS) data to different land cover types according to their spatial and spectral capabilities and then reduced or combined for later comparison purpose. The images belonging to various time intervals have different sensor performances investigating the change in the Land Use/Cover (LULC). In this case, the classification results will be different, because resolutions of sensors vary. Thus, the change analysis is preferred (Hashiba *et al*., 2000). The MSS sensor mounted on the landsat satellite collected data between 1972 and 1994, while the TM and ETM+ sensor have been in use and have aquired the image of the earth since 1982 and 1999 respectively.

Change detection with LANDSAT MSS data has been largely performed at mesoscale levels. The Landsat MSS sensor has 4 bands that simultaneously record reflected radiation from the earth's surface in the green, red, and near-infrared portions of the electromagnetic spectrum. The resolution for all bands of 79 m, the wave length is between 0.50-1.1 μm, and approximate scene size is 170 km north-south by 185 km east-west. Some results have been far from being satisfactory due to resolutions, where small changes and short time intervals failed to exhibit sufficient change to detect accurately with LANDSAT MSS data (Ridd *et al*., 1983).
Therefore, it is important to use other data sources such as topographic maps and aerial photographs besides high-resolution satellite images to evaluate the land use/cover changes.

The thematic mapper (TM) is an advanced, multispectral scanning, earth resources sensor designed to achieve higher image resolution, sharper spectral separation, improved geometric fidelity, and greater radiometric accuracy and resolution than that of the MSS sensor. The LANDSAT TM sensor has 7 bands, with a spatial resoulation of 30 meters for bands 1 to 5 and band 7 (wave length between 0.45-2.35 μm) that simultaneously record reflected or emitted radiation from the earth's surface in the blue-green, green, red, near-infrared, mid-infrared, and the far-infrared portions of the electromagnetic spectrum. Spatial resolution for band 6 (thermal infrared and wave length between 10.40-12.50 μm) is 120 meters, but band 6 data are resampled to 30 meter pixel size. Approximate scene size is 170 km north-south by 183 km east-west

Enhanced Thematic Mapper Plus (ETM+) is the successor of TM. The observation bands are essentially the same seven bands as TM, and the newly added panchromatic band 8, with a high resolution of 15m was added. Landsat ETM+ image data consist of eight spectral bands, with a spatial resolution of 30 meters for bands 1 to 5 and band 7 (wave length between 10.40-12.50 μm). Resolution for band 6 (thermal infrared and wave length between 10.40-12.50 μm) is 60 meters and resolution for band 8 (panchromatic and wave length between 0.52-0.90 μm) is 15 meters. Approximate scene size is 170 km north-south by 183 km east-west.

3.4. Hydrological models

Hydrological models are considered simplified representations of the real world where each model has its own conceptual approach and related mathematical formulation. In this study a rainfall-runoff is selected and serves to provide quantitative information of the catchment runoff and inherent characteristics. Understanding hydrological processes and their spatial and temporal patterns considered is basic for a sound water management. The application of hydrological models may help in various ways to understand and to assess future temporal distribution of water resources in the space and time dimension.

An important issue in modelling the hydrological response of a catchment is the level of detail at which land cover properties are represented, both where land cover patterns are stable and where they are changing over time. Nowadays, various approaches are available to assess the impacts of land cover changes in different parts of the world. Based on the assessment, most of the hydrological models belong to the categories of distributed physically based and semi distributed conceptual hydrological models. In this terminology physically based stand for the physiographic information of the catchment and climatic factors in a simplified manner while conceptual stands for the hydrologic state of a catchment, flow process at any time or instant.

Parkins (1996) described that the most rational way to model the impact of land cover changes on the runoff dynamics of a river catchment is through implementation of spatially distributed physically based hydrological models. In such approaches are land surface characteristics represented by land cover parameters and spatially organized in grid layers where parameters may be measurable to have physical meaning or simply be estimated and optimized through a procedure of model calibration. This class of models is highly demanding in terms of their data requirement and computational effort, which may increase further as the size of the catchment increases.

Semi-distributed conceptual approaches commonly are able to capture the dominating hydrological processes at the appropriate scale with accompanying formulations (see section 4.2). The conceptual models can therefore be considered as a compromise between the need for simplicity on the one hand and the need for a firm physical basis on the other hand. A disadvantage may be that it is generally impossible to derive the model parameters directly from field measurements and therefore calibration techniques must be used (Refsgaard, 1996).

Conceptual rainfall runoff (CRR) models are normally run with area and average values of precipitation and evaporation as primary input data and, subject to the selected approach, produces catchment values of soil-moisture, runoff volumes, peak flows etc.

Also in this study a CRR model is selected that on the one hand should be able to simulate catchment runoff with some assumed certainty but on the other hand does not require extensive data inputs to represents system properties. By its many effective applications the HBV rainfall-runoff model has been selected that basically solves the water balance for each model calculation time step as subject to inputs and outputs.

Other reasons why the HBV model is selected are the following:

- the input data requirement is moderate.
- the model simulates the major hydrological process in the catchment.
- the model was tested for hydrological responses to land cover change study in different parts of the world and
- the availability of the model

.

4. METHODOLOGY

4.1. Image processing

Landsat satellite imageries were used in this study to identify changes in land cover distribution in the Upper Gilgel Abbay catchment over a 28 years period from 1973-2001. Three images were selected for land cover mapping of Gilgel Abbay catchment. Landsat MSS, TM and ETM+ were selected to represent the land cover conditions in the years 1973, 1986 and 2001 respectively. The images are particularly acquired for the dry season to capitalize on a) the pronounced difference in reflectance between forested and non forested areas, b) decreasing confusion at forest edges between dense forest vegetation and small scale agriculture plots. The images provide complete coverage of Upper Gilgel Abbay catchment. For the extraction of elevation, drainage network and catchment boundary a SRTM-DEM of the year 2000 was selected. For the year 1999 a Normalised Difference Vegetation Index (NDVI) map from a Landsat image was processed to identify agriculture and grass land as shown in figure 4.2. The Landsat image was selected since only 20 % of the catchment was covered by cloudy, and also the acquisition date of the image was Sept.12, 1999.

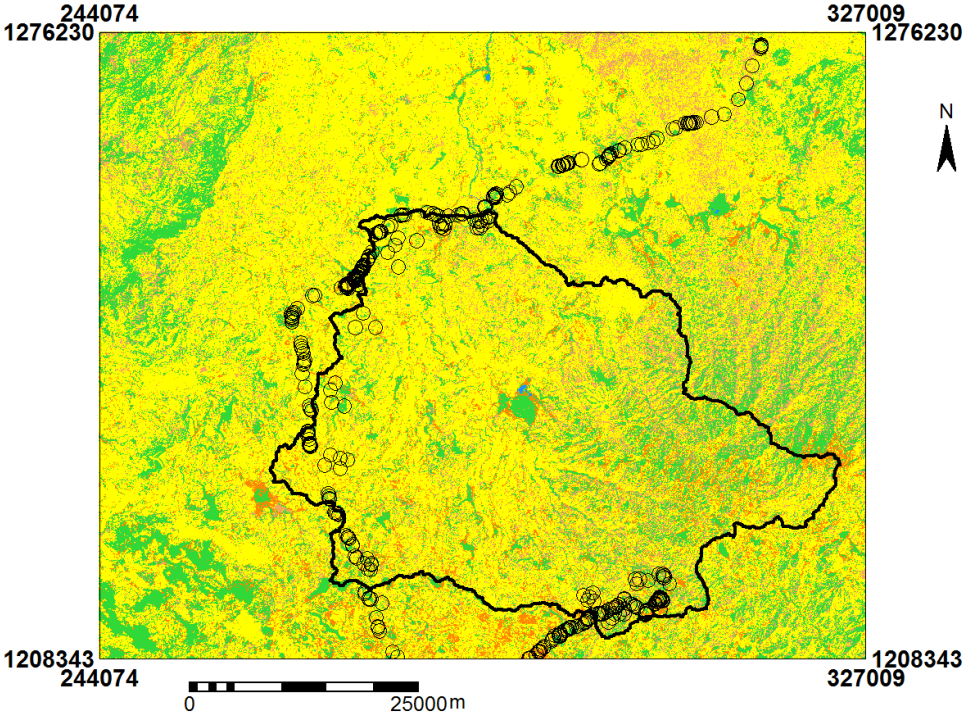

Figure 4-1: Locations of ground control points

Three orthorectified images for 1973, 1986 and 2001 were provided by NASA and Global Land cover Facility (GLCF). As indicated in figure 4.1, a large number (i.e. 498) of ground control points (GCP) were available for the training and accuracy assessment where 80% of the data points were used for training and 20% for accuracy assessment. The image of 2001 was georefenced using ground control points collected by GPS during the field campaign, and 1:50,000 scale topographic map of the study

area. The root mean square error (RMSE) the first order polynomial function (affine transformation) was found to be 0.20 pixel (or 0.6 m on the ground). The two other date images (1973 and 1986) were then rectified to the georefenced image by image to image registration method. Image registration is the process of making an image to conform to another image and involves georeferencing if the reference image is already rectified to a particular map projection. Thus to allow for spatial comparison of images through change detection, image to image registration is usually used for the time series data like multi-temporal images over the same region in order to place the same coordinate system to separate images. In general, RMSE limit for the change detection on land cover is preferred less than 0.50 pixel when registering the images. Therefore, the 1973 and 1986 images were registered to the 2001 image by image to image registration with an RMSE of registration was found to be 0.34 pixel (or 19.38m on the ground) for the 1973 image and 0.22 pixel (or 6.6 m on the ground) for the 1986 image. The total root mean square errors (RMSE) of the registered images were quite low to accept the limit required for the change detection. All images were rectified to UTM projection, WGS 1984 datum and Zone 37N for the purpose of analysis.
Since images are observed at different moments in time different conditions prevailed in the atmosphere and haze and dust can mask actual changes of land cover. Work by Huete and Tucker (1991) indicates that atmospheric conditions significantly may affect the vegetation coverage of the catchment, and thereby influence through the normalised difference vegetation Index (NDVI). As such the satellite images have been corrected for these atmospheric effects while ATCOR (atmospheric correction software) which is embedded in ERDAS Imagine software has been selected to correct the atmospheric effects on the images.

Table: 4-1 shows the acquisition dates, sensor, path/row, resolution and the producer's of the Images. Since the image had different file format, all images were imported in ILWIS and the tagged file formats (TIF) was selected. For atmospheric correction, the images were exported into ERDAS using the Erdas.LAN file format.

Table 4-1: The data source for the analysis of change in land cover

[Path/Row]	Sensor	Acquisition date	Resolution (m)	Producer's
183/52	MSS	Feb 01, 1973	57	GLCF
170/52	TM	Jan 03, 1986	30	GLCF
170/53	ETM+	Feb 05, 2001	30	GLCF
170/54	ETM+	Sept 12, 1999	30	GLCF
	SRTM	2000	90	USGS/GLCF

4.2. Land cover mapping

4.2.1. Land cover class

After the observation during the field work five different types of land cover have been identified for the upper Gilgel Abbay catchment. The description of these land covers are given as follows:

Forest Land: Area with high density of trees which include deciduous forest land, ever green forest land, mixed forest land and plantation forests that mainly are eucalyptus, junipers and conifers.

Agriculture: Areas used for both annual and perennial crop cultivation, and the scattered rural settlements that are closely associated with the large sized cultivated fields. Due to the difficulty encountered in identifying the dispersed rural settlements this type of land cover was combined with the cultivated land during classification.

Shrubs land: Areas covered with shrubs, bushes and small trees, with little wood, mixed with some grasses.

Grass land: Area covered with grass that is used for grazing and that is equal to remain grass cover for a considerable period of the year (half of the year).

Water and marshy land: Area which remains water logged and swampy throughout the year, the man made water harvesting ponds, the rivers and its main tributaries.

4.2.2. Image classification

Effective classification of remote sensing image data depends upon separating land cover types of interest into sets of spectral classes (signatures) that represent the data in a form suited to the particular classifier algorithm used (Richards & Kelly, 1984).In this study, land cover for the selected date was estimated using the supervised image classification.

For the supervised classification, the ground control points collected in the field were used as the training sample set. Supporting information was obtained from field observation of the land cover, interviews with local elder people and topographic maps. The sample set was created using the band combination of 7, 4, 2 (images of 1986 and 2001) and 4, 2, 1 (image of 1973) for visual interpretation of the image in their true colour. MSS sensor bands (1, 2, 3, and 4) have the spectral range between 0.45-1.10 µm. Both TM and ETM+ sensor bands (1, 2, 3, 4, 5, and 7) also have the spectral ranges between 0.450-2.5µm. Bands 1–3 represent visible electromagnetic radiation with wavelengths 0.45–0.52, 0.52–0.60, and 0.63–0.69 µm, respectively. Band 4 represents near infrared with wavelengths of 0.76–0.90µm, and bands 5 and 7 represent mid-infrared with frequencies of 1.55–1.75 and 2.08–2.35 µm, respectively.

The classification was performed by assigning the pixels to what land cover class they belong in the sample set. In the classification, the maximum likely hood classifier was used that is the most widely used in image classification. The algorithm was selected since unlike other classifiers it considers the spectral variation within each category and the overlap that may occur among different classes (Campbell, 2002). This is also achieved by calculating a statistical distance based on the mean values and covariance of the clusters. The spatial coverage of each land cover class can be visualized on three of historical land cover map. In general, a total of five major land cover classes were selected in this catchment: agricultural land, grass land, shrubs land, forest land, and water and marshy land.

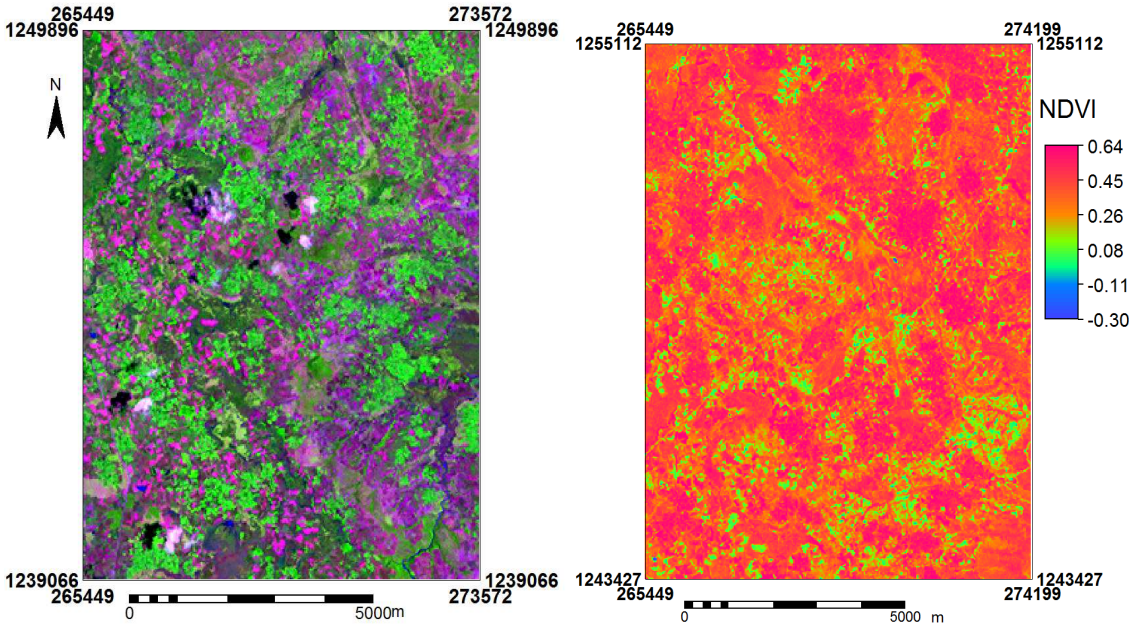

Figure 4-2: NDVI map of Gilgel Abbay catchment partly (ETM+, 1999)

4.2.3. Accuracy of image classification

Accuracy assessment is an important step in the image classification process. The objective is to quantitatively determine how effectively pixels were grouped into the correct features classes in the area under investigation. The confusion matrix as derived from the image map and filed data was generated for accuracy assessment.

The overall accuracy is evaluated as the total number of correctly classified pixels (diagonal elements) divided by the total number of ground truth pixels. User's accuracy and producer accuracy measured the correctness of each category with respect to errors of commission and omission. The user's accuracy is defined as the probability that a reference pixel has been correctly classified as well as the producer accuracy is defined as the probability that a pixel classified on the map represents that class on the ground (Anderson, 1976). A lower user's accuracy represents a high error of commission while a low producer's accuracy represents a high error of commission.

The accuracy of thematic maps was determined by the constructed matrices along kappa statistics in order to test whether any difference exists in the interpretation. Briefly, kappa statistic considers a measure of overall accuracy of image classification and individual category accuracy as a means of actual agreement between classification and observation. The value of kappa lies between 0 and 1, where 0 represents lack of agreement between classification and observation. Meanwhile 1 represents complete agreement between the two data sets. A Negative value would mean worse agreement than expected by chance.

Generally, the maximum likelihood estimate of Kappa was computed as follows:

$$k = \frac{p_o - p_c}{1 - p_c} \tag{4.1}$$

Where:

Po - The proportion of observed agreements

Pc - The proportion of agreements expected by chance

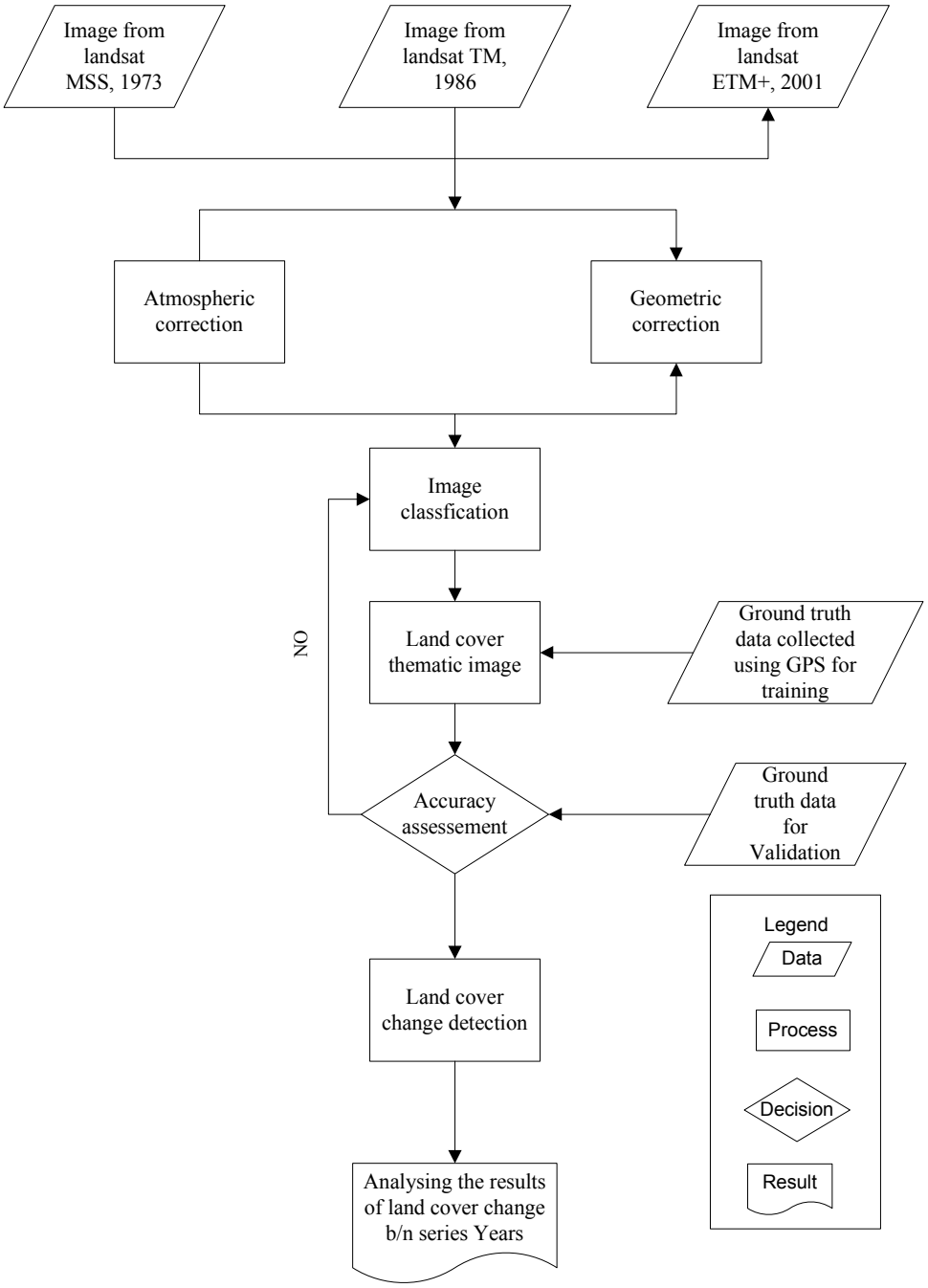

4.3. Hydrological modeling (HBV 96)

4.3.1. General description

A daily discharge record of Upper Gilgel Abbay river was simulated interims of the historical land cover changes by using HBV-96 model for the period of 1973−2005. The HBV-96 model is a mathematical model and was designed originally to apply for runoff simulation and hydrological forecasting. This model can also be used for water balance studies, for runoff forecasting, to compute design flood for dam safety, to assess and simulate hydrologic responses due to the effects of land cover change and climate change (Seibert, 2002).

The general water balance model is described as:

$$P - E - Q = \frac{d}{dt}[SP + SM + UZ + LZ + lakes] \quad (4.2)$$

Where: P: precipitation, SP: snow pack, UZ: upper ground zone, LZ: lower ground zone, Q: runoff, E: evapotranspiration, SM: soil moisture, Lakes: lake volume.

4.3.2. Model structure

The HBV-96 is described as a semi-distributed conceptual model that allows dividing the catchment into sub basin and the sub basins further divided into elevation and vegetation zones. The model simulates daily discharge using daily rainfall, temperature and estimates of average monthly potential evapotranspiration as input together with geographic information about the catchment.

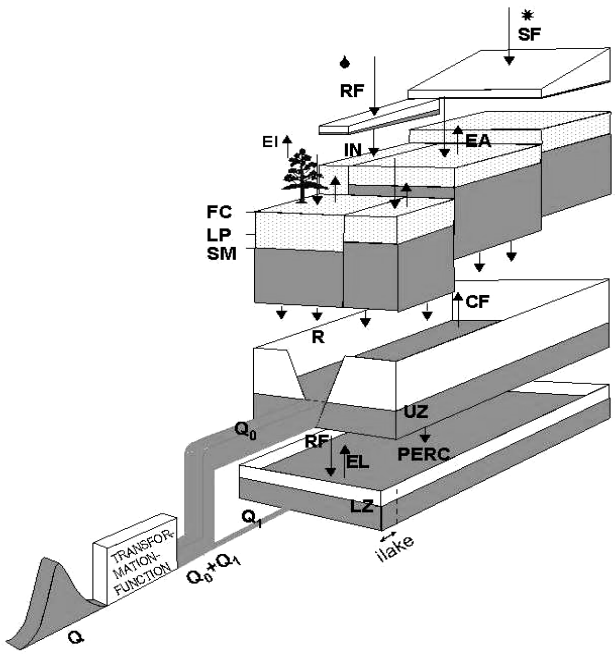

Figure 4-3: Schematic structure of HBV-96 model (SMHI, 2006)

Where: EA: actual evapotranspiration, EI: evaporation from interception, SM: soil moisture storage, FC: maximum soil moisture storage, LP: limit for potential evapotranspiration, β: soil parameter, PERC: percolation, K_4: recession parameters, α: recession parameter, RF: rainfall, IN: infiltration, SF: snow factor, Q_O+Q_1: runoff components, KHQ: recession at HQ, UZ and LZ storage in upper and lower response box respectively.

The model was run for each of five subbasins separately and was combined from all subbasins. Calibration was done at the outlet of Wotet Abbay gauged station. The overall effect of elevation zone with respect to different vegetation zone (forested and non- forested) was also considered by dividing the catchment into five subbasins.

The model consists of subroutines for precipitation and snow accumulation, for soil moisture accounting where ground water recharge and actual evaporation are coupled, and it consists of response routines, a transformation function and a simple routing procedure.

Soil routine

Soil moisture routine is based on three parameters β, LP and FC. β controls the contribution to the response function and the increase in soil moisture storage, LP is the soil moisture value above which evapotranspiration reaches its potential value and FC is the maximum soil moisture storage in the model. The soil moisture is expressed as follows:

$$\frac{\Delta Q}{\Delta p} = \left(\frac{SM}{FC}\right)^{\beta} \tag{4.3}$$

The relation between the soil moisture and evapotranspiration in HBV model can also be expressed as (Seibert, 1997):

$$Ea = Ep\left(\frac{SM}{LP * FC}, 1\right) \tag{4.4}$$

Where:

SM	- computed soil moisture storage
ΔP	- contribution from rainfall
ΔQ	- contribution to the response function
FC	- maximum soil moisture storage
β	- Empirical coefficient
E_p	- potential evapotranspiration
E_a	- compute actual evapotranspiration
LP	- limit for potential evapotranspiration

Response routine

The runoff-response function is used to transform excess water from the soil moisture zone runoff. The routine consists of one upper reservoir and one lower reservoir. The storage in the upper reservoir will receive the yield from the soil moisture zone. That is if the yields from the soil moisture routine exceed its percolation capacity, the upper reservoir starts to fill. By then the water will percolate to the lower reservoir. The lower reservoir conceptually represents the ground water that contributes to the base flow of the catchment.

The outflow from the upper reservoir is described as follows:

$$Q_o = k * UZ^{(1+\alpha)} \tag{4.5}$$

The outflow from the lower linear reservoir is described as follows:

$$Q_1 = k4 * LZ \quad (4.6)$$

Where: Q_o: Direct runoff from upper reservoir, k: recession coefficient upper reservoir storage, Q_1: lower reservoir out flow, LZ: lower reservoir storage and k4: recession coefficient of lower reservoir storage.

Generally, the soil routine parameters FC, LP, and β characterizes to influence the total volume, where as the response parameters, k4, perc, khq, Hq and alfa influence the shape of the hydrograph rather than the total volume. Since Hq is not calibrated, its value was calculated as follows:

$$Hq = \frac{(MQ * MHQ)^{1/2} * 86.4}{A} \quad (4.7)$$

Where:

MQ - Mean of the observed discharge flow over the whole period (m^3/s)

MHQ - Mean annual peak flows (m^3/s)

A - Area of the catchment (Km^2)

The value of MQ, MHQ for the period of 1999-2003 and area of the catchment are tabulated as:

MQ (m^3/s)	MHQ (m^3/s)	A (Km^2)
50.861	334.492	1656.12

Therefore, the calculated value of Hq for upper Gilgel Abbay river is 6.61 mm/day.

The parameters K4 and perc were used to calibrate base flows during the period of low flows. The low value of perc results in a low base flow, and K4 describes the recession of base flow. For the calibration of peak flow during high flow periods, the parameters Khq and alfa were used. A higher Khq results in higher peaks and a more dynamic response in the hydrograph. The higher alfa triggers the higher peaks and quicker recession.

4.3.3. Model input

The model input requirements for the HBV model are daily rainfall, temperature, estimate of average monthly potential evapotranspiration and catchment characteristic of the study area.

Areal rainfall

As the HBV model requires daily rainfall as an input, it was prepared from the data of meteorological stations within and adjacent to the upper Gilgel Abbay river basin. A total of eight rainfall stations is

used inside and close to the catchment are used to estimate the rainfall amount. Two stations Wotet and Sekela are located inside the catchment while the six of stations Dangila, Inijibara, Kidimaja, Adet, Gundil and Abbay Shelko are located outside or around the catchment. A daily areal rainfall of catchment was calculated from daily point measurement of meteorological stations by using the Thiessen polygon and Inverse distance methods (sees equation 4.8) and (sees equation 4.9).

Thiessen polygon method

The Thiessen polygon method is one way of calculating areal precipitation. This method gives weight to station data in proportion to the space between the stations. The area of each polygon inside the subbasin, as a percentage of the total subbasin area, is calculated. This factor is then used as the weight of the station situated within that polygon. The Theissen weight for each station was calculated for each subbasin in table 4.2. The precipitation for the whole area is then calculated as follows:

$$\overline{P} = \frac{1}{A_{TOT}} * \sum_{j=1}^{k} AjPj \qquad (4.8)$$

Where:

$\overline{P}$ - Average areal rainfall

Pj - Rainfall measured at each station

Aj - Area of each polygon inside the basin

A_T - Total subbasin area.

Table 4-2: Weight of meteorological station by Theissen polygon method.

	Subbasins				
Stations	Subbasin 1	Subbasin 2	Subbasin 3	Subbasin 4	Subbasin 5
Dangila			0.44	0.00	0.24
Sekela	0.89	0.14		0.49	
Wotet	0.07	0.85		0.04	0.68
Adet	0.04	0.01			
Kidimaja			0.03		
Inijibara			0.52	0.11	0.01
Shelko					0.08
Gundil				0.36	

Inverse distance method

The rainfall intensity at a point P(x,y) outside rain gauge network is inversely proportional to distance. I.e. a rainfall station nearer to the interpolated point has a larger weight compared to the station which is at large distance. For this study the centre of catchment was considered in the interpolation and applied to the whole subbasin to compute the weight of each station as is shown in table 4.3. The power parameter n controls how the weighting factor reduces as the distance from the reference point increases in equation (4.2), and the power parameter n=2 was used for this study. The equation for calculating the spatial average rainfall is calculated as follows:

$$\overline{P} = \frac{\frac{1}{di^n} Pi}{\sum_{i=1}^{k} \frac{1}{di^n}} \qquad (4.9)$$

Where:

$\overline{P}$ = Average areal rainfall

Pi = Rainfall measured at each station.

di = Distance of stations from the centre of subbasin

n = Power parameter or weight

k = Number of meteorological stations

i = Minimum number of meteorological station.

Table 4-3: Weight of meteorological station by inverse distance method.

	Subbasins				
Stations	Subbasin 1	Subbasin 2	Subbasin 3	Subbasin 4	Subbasin 5
Dangila	0.06	0.09	0.27	0.05	0.2
Sekela	0.35	0.16	0.05	0.37	0.05
Wotet	0.11	0.28	0.08	0.06	0.41
Adet	0.17	0.15	0.02	0.04	0.03
Kidimaja	0.05	0.05	0.16	0.05	0.05
Inijibara	0.07	0.07	0.24	0.1	0.06
Shelko	0.14	0.11	0.1	0.28	0.06
Gundil	0.05	0.09	0.08	0.04	0.15

In general, the inverse distance weighted method gives better result and it takes into account the contribution of rainfall from each station to the whole subbasin. Therefore, this method was adopted for this study.

Catchment data

In hydrologic modelling the first step is to delineate the catchment of the study area and then to discretize to hydrologic response units. The concept of HRU is capable of preserving the heterogeneity of the three – dimensional physiographic properties of the drainage basin (Flugel, 1995). The delineation of HRU is done on the basis of characteristics such as slope, aspect, elevation, vegetation-type, soil type and distribution of precipitation. Each hydrologic response is assumed to have homogenous hydrologic characteristic. The distributed parameter to analyse the effect of heterogeneity of the river basin it was divided into five subbasins as shown in figure 4.5. The subbasins are classified into elevation in to elevation range and again into different vegetation zones. This was done by preparing the Digital elevation Model (DEM) using Shuttle Radar Topography Mission (SRTM) with 90m resolution (see in figure 2.2) together with different period of land cover map (see section 5.2). Elevation zones were considered as primary hydrological units of the catchment and were divided into different vegetation zones

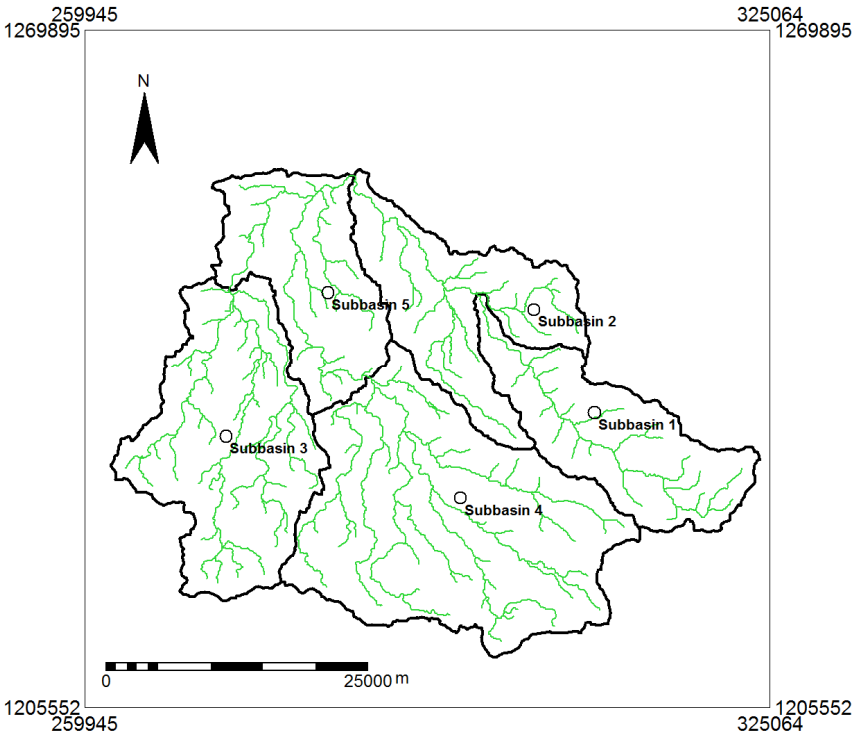

Figure 4-4: Upper Gilgel Abbay river basin divided in to five subbasins

The result of land cover assessment (see section 5.1) indicated that they are five major land cover class is in the catchment. However, for this study area, the HBV-96 model considers the forested land cover as a unit and the non-forested land cover that is termed as one unit “field”. The zonations were done based on elevation and land cover data of each subbasin. During the whole period of study, the

largest forest and field land cover zone were found at subbasin 4, and it is the highest elevated area next to subbasin 1. Land cover zones in each subbasin for three different periods are summarized as shown in table 4.4, 4.5 and 4.6.

Table 4-4: Land cover zones and area coverage in each subbasin for the year 2001

Subbasin Name	Elevation (m)	Land Cover Zone		Total area (Km^2)
		Field (Km^2)	Forest (Km^2)	
Subbasin1	2738.9	170.51	69.43	239.94
Subbasin2	2281.6	213.10	33.17	246.27
Subbasin3	2425.3	326.79	45.29	372.08
Subbasin4	2541.8	456.99	108.71	565.70
Subbasin5	2052.1	210.54	21.56	232.11

Table 4-5: Land cover zones and area coverage in each subbasin for the year 1986

Subbasin Name	Elevation (m)	Land Cover Zone		Total area (Km^2)
		Field (Km^2)	Forest (Km^2)	
Subbasin1	2738.9	108.38	132.78	241.16
Subbasin2	2281.6	57.05	192.30	249.34
Subbasin3	2425.3	104.79	264.75	369.54
Subbasin4	2541.8	228.95	333.07	562.01
Subbasin5	2052.1	45.04	189.03	234.08

Table 4-6: Land cover zones and area coverage in each subbasin for the year 1973

Subbasin Name	Elevation (m)	Land Cover Zone		Total area (Km^2)
		Field (Km^2)	Forest (Km^2)	
Subbasin1	2738.9	87.56	152.13	239.69
Subbasin2	2281.6	128.19	122.34	250.53
Subbasin3	2425.3	230.53	140.19	370.58
Subbasin4	2541.8	231.49	328.63	560.13
Subbasin5	2052.1	134.70	100.51	235.21

Evapotranspiration

The HBV model requires monthly data of long-term mean potential evapotranspiration (SMHI, 2006). There are number of methods to estimate evapotranspiration and they are based on specific climatic variable required for calculation. In this study daily potential evaporation is calculated by using Penman-Monteith formula in equation (3.3). The penman approach of estimating evapotranspiration combines the mass transfer and energy-balance approaches because of which it gained strong physical base (Dingman, 2002). The FAO Penman Monteith method requires radiation, air temperature, air humidity, and wind speed data.

$$ET_o = \frac{0.408\Delta(Rn - G) + \gamma \frac{900}{T + 273} U2(es - ea)}{\Delta + \gamma(1 + 0.34U2)} \quad (4.10)$$

Where

ETo = Reference evapotranspiration [mm day^{-1}]

Rn = Net radiation at the crop surface [MJ m^{-2} day^{-1}]

G = Soil heat flux density [MJ m^{-2} day^{-1}]

T = Mean daily air temperature at 2 m height [°C]

U2 = Wind speed at 2 m height [m s^{-1}]

Es = Saturation vapour pressure [kPa]

ea = Actual vapour pressure [kPa]

Δ = Slope vapour pressure curve [kPa °C-1]

γ = Psychometric constant [kPa $°C^{-1}$].

4.3.4. Model Calibration and Validation

By model calibration, which stands for the fine-tuning of the input parameter data, the performance of the model will be improved. Hydrological models require the procedure of adjusting values of the model input parameters to match model output with measured field data for the selected period and situation entered to the model (Rientjes, 2007).

There are three major approaches for calibrating the model in order to identify the optimum parameter set. These are manual calibration, automatic calibration, and calibration through Monte Carlos simulation. Among these methods the manual calibration was applied for this study. Under this approach the user adjust the parameters interactively in successive model simulations. Advantage of this approach is the dependency of the user, since it builds on accumulated experience and only intelligent steps through the parameter space will be made. The weakness of this approach is there is no clear point at which the calibration process can be said to be completed. But what is possible is relative judgment based on the objective function. The model was also validated against an independent data with forcing terms which was not used during calibration to test the model simulation capability. Generally the model was evaluated through the goodness of fit of the simulated to the observed runoff can be assessed by three different criteria:

- Visual inspection of the computed and observed hydrographs i.e. a good overall agreement of the shape of the hydrograph.
- Calculating the volume error using equation (4.11). This volume error can vary between ∞ and - ∞ but performs best when a value of zero is generated since no difference between simulated and observed discharge occurs. A relative volume error less than +5% or −5% indicates that a model performs well while relative volume errors between +5% and +10% and −5% and −10% indicates a model with reasonable Performance.

$$RV_E = \left(\frac{\sum_{I=1}^{N} Q_{sim(i)} - \sum_{i=1}^{n} Q_{obs(i)}}{\sum_{i=1}^{n} Q_{obs(i)}} \right) 100\,\% \qquad (4.11)$$

Where

RV_E - Relative volume error

$Q_{sim(i)}$ - Simulated flow

$Q_{obs(i)}$ - Observed flow

- Evaluating the efficiency of the model by relating the goodness fit of the model to the variance of the measured data through Nash-Sutcliffe coefficient, R^2 (see equation 4.12). The Nash-Sutcliffe coefficient ranges from 0 to 1, expressed in the equation here which is used to evaluate the performance of the model. A value of 1.0 represents perfect performance.

Further, it is known that a value between 0.6 and 0.8 indicates that the model performs reasonably. Values between 0.8 and 0.9 indicate that the model performs very well and values between 0.90 and 1.0 indicate that the model performs extremely well (Nash and Sutcliffe, 1970).

$$R^2 = 1 - \frac{\sum_{i=1}^{n}\left(Q_{sim(i)} - Q_{obs(i)}\right)^2}{\sum_{i=1}^{n}\left(Q_{obs(i)} - \overline{Q}_{obs}\right)^2} \qquad (4.12)$$

Where:

R^2 – Nash-Sutcliffe coefficient

$Q_{sim(i)}$ – Simulated flow

$Q_{obs(i)}$ – Observed flow

$\overline{Q}$ – Mean of observed flow

During the development of the model, seven years of the data (1999-2005) was divided in to three. Before calibration, the first year of data (1999) was used to warm up of the mode for initialization. For calibration and validation of the model the remaining data was used from the period of 2000-2003 and 2004 -2005 respectively.

4.3.5. Effects of land cover change on the river system

To assess the effects of land cover change on the hydrologic response of the catchment, simulated stream flow corresponding to historical land cover was done using the HBV model which was calibrated and validated as discussed in the previous section. Rainfall and evaporation data of four years (2000−2003) were used during simulation. The model meteorological forcing terms (rainfall, evapotranspiration) were also kept constant during the period of 1973, 1986 and 2001 for which the land cover map that processed in this study. Only the land cover parameters were changed so as to eliminate their effects on the stream flow. Due to the fact that mentioned in the above the effects of land cover change on the basin hydrology was separated from the effects of variable climate in the catchment. The result of simulation was evaluated by the following two general procedures. First, by visually inspecting the three simulated hydrographs were compared to peak flows, base flows and the recession using the daily, monthly and annual means. Second, the temporal variation of flows, peak flows and base flows were used to compare the three simulated hydrographs during the period of wet season and dry season respectively.

.

5. RESULT AND DISCUSSION

5.1. Land cover classfication

5.1.1. Accuracy assessment

To access the accuracy of the classified image, a confusion matrix was constructed by using the additional ground truth information (ground control points) which was not used in the training classification. Totally 100 ground control points were used to validate the classified image. Since the field data is not available for the 1973 and 1986 images, the accuracy assessment was performed only for the 2001 image. The accuracy of the 2001 land cover map is shown in table 5.1.

The overall accuracy that is the user's accuracy, producer's accuracy, and the kappa statistic were, and then derived from the error matrix. The overall accuracy of the classification was 83 % with kappa coefficient of 0.78. The kappa statistic was calculated from the result of the land cover classification, with five classes shown at the bottom of the confusion matrix table. This implies that the kappa value of 0.784592 represents a probable 75 percent better accuracy than if the classification resulted from a random unsupervised classification, instead of maximum likelihood classification. Landis (1986) defined the agreement criteria for kappa statistic, the agreement is poor when $k < 0.40$, good when $0.4 < k < 0.7$ and excellent when $k > 0.75$. Alternatively, Monserud (1990) suggested the use of subjective kappa value as < 40 % as poor, 40-55 % fair, 55-70 % good, 70-85 % very good and > 85 % as excellent. Thus, according to these classification scales, the classification for this study denotes very good to excellent agreement.

For the average accuracy and average reliability the results were 82.88 % and 84.07 % respectively. Producer's accuracy values for all class except shrubs ranged from 80-90%. The values indicate that the landsat data and the methodologies employed in this study allowed for the land cover identification of the majority of reference points as belonging to one of the selected classes.

Table 5-1: Confusion matrixes for validation of land cover map 2001

	Classified data					
Reference Data	WM	AG	GL	F	WM	Producer's accuracy, %
WM	12	0	2	0	0	85.71
AG	0	22	2	2	0	84.62
GL	1	2	17	0	0	85.00
F	0	1	1	19	2	82.61
WM	0	2	0	2	13	76.47
User's accuracy, %	92.31	81.48	77.27	82.61	86.67	
Over all classfication accuracy = 83 %						
kappa statistic = 0.78						

Note: WM= Water and marshy land, AG= Agricultural land, GL= Grass land, F= Forest, SL= Shrubs land.

5.2. Land cover map

The land cover map of 1973 in figure 5.2 and the histogram of the land class coverage in figure 1.2 shows that about 51% of the upper Gilgel Abbay catchment was covered by forest, 17% by shrubs land, 28% by agriculture land, 4% by grass land and very little by water and marshy land. The distribution of land cover class as it is shown in the figure 5.1, forest cover was found in most parts of the catchment; especially the south eastern part of the catchment is more dominantly covered by forest. These areas have a terrain of mountains and steep slope characteristics. During this period most of the population was settled in the lower elevated areas (north and south western part of the catchment) and there was some activity of agriculture.

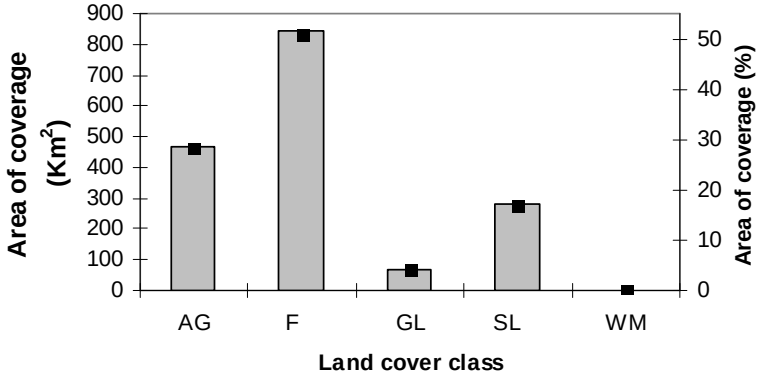

Figure 5-1: Histogram of land cover class coverage in 1973

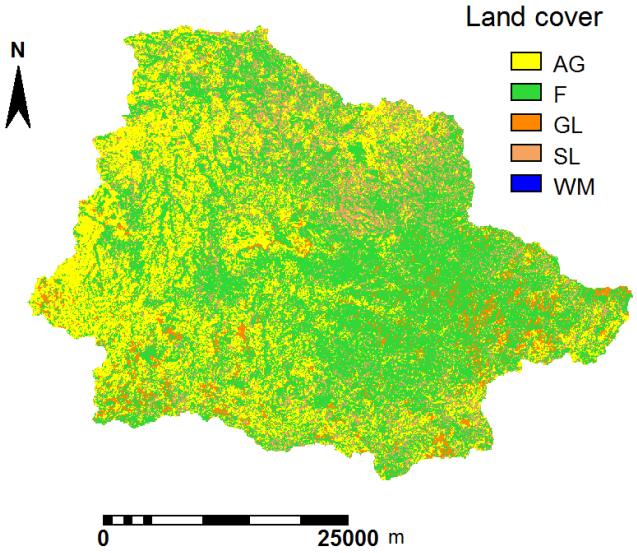

Figure 5-2: Land cover map of Upper Gilgel Abbay catchment in 1973

The land cover map of 1986 in figure 5.3 and the area coverage of each land cover class in figure 5.4 show that the catchment was covered by 33% forest, 40% agriculture, 13 % grass land, 13% shrubs land, and 1% of water and marshy land. During this period, mainly the forest in the Northern,

Western, South-Western and the central part of the catchment was reduced. On contrast the agriculture was expanded in most parts of the catchment. This is due to the population growth and settlements in higher elevated or mountains area where forests are cleared.

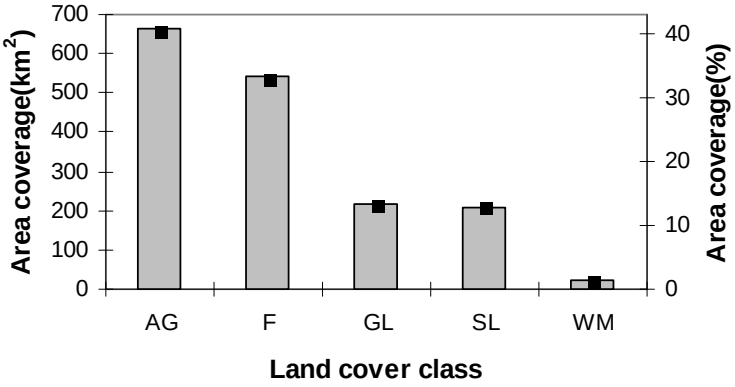

Figure 5-3: Land cover map of Upper Gilgel Abbay catchment in 1986

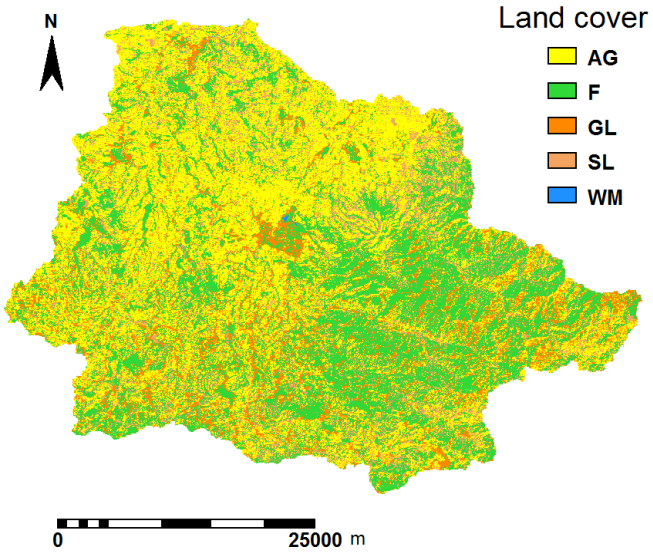

Figure 5-4: Histogram of land cover class coverage in 1986

For the year 2001 the land cover map is shown in figure 5.6.The area coverage of each class is shown in figure 5.5 and indicates that agricultural land covered some 62% while forest, shrubs land, grass land, water and marshy land covered 17%, 9%, 9% and 3% respectively. During this period and due to high increase of population density, this caused scarcity of agriculture in low land areas that necessitated many of them to settle in sloppy or mountainous areas. As a result most of the catchment area was transformed into agricultural lands, and only little forest cover remains through the South-Eastern part of the catchment.

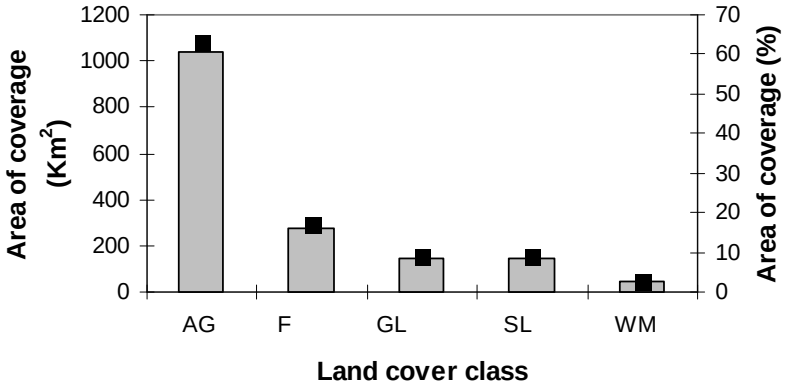

Figure 5-5: Histogram of land cover class coverage in 2001

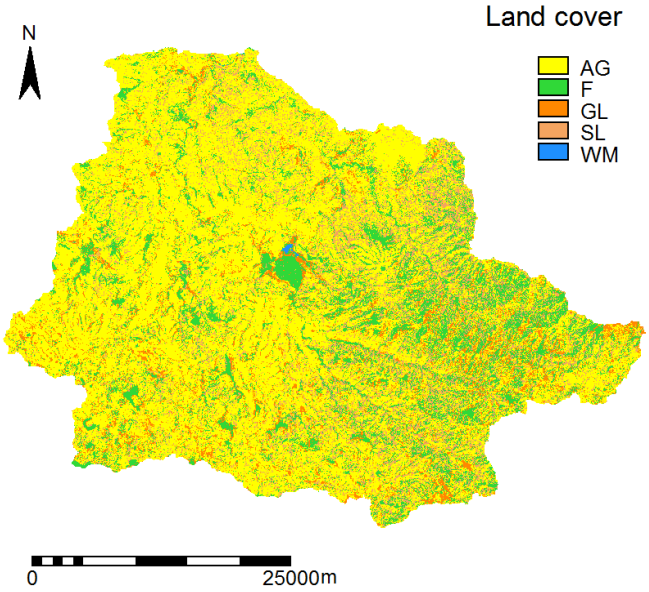

Figure 5-6: Land cover map of Upper Gilgel Abbay catchment in 2001

5.3. Summary of land cover class

Land cover classification maps of the study area were generated for three reference years 1973, 1986 and 2001 and reflect land cover for dry season periods. The individual class areas and change statistics for the period of 1973 to 2001 are summarized in table 5.2 and table 5.3, respectively.

Table 5-2: Summary of land cover type in Upper Gilgel Abbay catchment for 1973, 1986 and 2001.

	1973		1986		2001	
Land cover Types	Km^2	%	Km^2	%	Km^2	%
GL	65.7	4.0	215.9	13.0	146.5	8.8
SL	279.4	16.9	209.9	12.7	147.5	8.9
WM	0.1	0.0	20.5	1.2	45.8	2.8
F	843.8	50.9	544.2	32.9	277.4	16.7
AG	467.2	28.2	665.62	40.2	1038.9	62.7

Note: WM= Water and marshy land, AG= Agricultural land, GL= Grass land, F= Forest, SL= Shrubs land.

Table 5-3: Summary of land cover changes in the Upper Gilgel Abbay catchment for the period of 1973-1986 and 1986-2001.

	1973−1986		1986−2001	
Land cover types	Km^2	%	Km^2	%
GL	150	9	-69.36	-4
SL	-69.54	-4	-62.32	-4
WM	20.33	1	25.29	2
F	-299.67	-18	-266.71	-16
AG	198.59	12	373.17	23

Note: WM= Water and marshy land, AG= Agricultural land, GL= Grass land, F= Forest, SL= Shrubs land.

In table 6.3 the negative and positive sign indicates the decrease and increase respectively of land cover class for the specified time period.

During the period of 1973-1986, agriculture area has increased approximately by a rate change of 0.92% per annum, while forest decreased by 18% with a rate change of 1.38% per annum. These changes showed that the deforestation increased and that forest land changed into agricultural and grass lands in the catchment.

During the period of 1986-2001, the agriculture area increased to 23% with a rate of change of 1.53% per annum, while the forest decreased by 16% with a rate of change of 1.07% per annum. Generally there is an increase in the water and marshy area in the catchment in this period. The increase of man made water harvesting pond in the catchment may have caused the increased in coverage of water and marshy lands.

Over the past 28 years, almost all of the agricultural expansion has resulted from the deforestation where forest lands are cultivated so become agricultural land. Therefore, in the year 2001 approximately 70% of forests were destructed within the reference period.
This is Body text style. Use this for the body text.

5.4. Change detection

To assess the land cover change through post classification and matrix analysis between the years 1973 and 1986, the 30m images was resampled to 57m by using the nearest neighbourhood technique as discussed in section 4.1. The results of the statistical change analysis of the study area are shown in table 5.4 and 5.5. Note that the matrix table 5.6 and 5.7 may read as the total area cover of land cover class in 1973 (correspond to the row) converted into different land cover class in 1986 (correspond to the column value). For example: the first row of table 5.6 (GL), the total area of land cover is 65.7 Km^2 .This value was converted into 6 Km^2 SL, 5Km^2 WM, 5Km^2 F and 10 Km^2 AG during the period of 1986. Area of land cover without changes are located a long the major diagonal of this matrix

Table 5-4: Land cover (LC) conversion matrix (km^2) for the period 1973 and 1986.

		1986					
	Land cover types	GL	SL	WM	F	AG	1973
	GL	41	6	5	5	10	65.7
	SL	13	83	5	60	118	279.4
1973	WM	0	0.1	0	0	0	0.1
	F	95	68	0	414	267	843.8
	AG	67	54	10	66	271	467.2
	1986	216	210	20	545	665	1656

Note: WM= Water and marshy land, AG= Agricultural land, GL= Grass land, F= Forest, SL= Shrubs land.

Table 5-5: Land cover (LC) conversion matrix (km^2) for the period 1986 and 2001

		2001					
	Land cover types	GL	SL	WM	F	AG	1986
	GL	61	6	23	27	99	65.7
	SL	18	76	0	16	100	279.4
1986	WM	10	0	9	0	1	0.1
	F	30	23	2	192	299	843.8
	AG	29	43	11	43	538	467.2
	2001	146	210	20	277	1039	1656

Note: WM= Water and marshy land, AG= Agricultural land, GL= Grass land, F= Forest, SL= Shrubs land.

In the change detection analysis, it can be stated that a comparatively significant variation in land cover occurred between the years 1973 and 2001. Table 5.4 and Table 5.5 demonstrate the kind of land cover change, namely “from- to” information that occurred between 1973 -1986 and 1986 - 2001, respectively.

As it is shown in Table 5.4, 267 km^2 forest areas was converted into agriculture land during the period 1973-1986.The agriculture land was expanded almost three and half times in 1986. Similarly from the total of forest cover in 1973, 414 km^2 of it was conserved; 68 km^2 of it was converted into shrub land and 95 km^2 to grass land. On the other hand, 5km^2 of grass land, 60 km^2 shrubs land and 66 km^2 of agriculture land was reforested during this period.

Between 1986 and 2001, the statistics provided in table 5.5 indicate that a total decrease of 268 km^2 of forest was occurred; 30 km^2 of it was converted to grass land, 23 km^2 to shrubs land, and 2 km^2 to water and marshy land. In contrast, 27 km^2 grass land, 16 km^2 shrubs land, and 43 km^2 agricultural land was gained as forest area in the catchment.

During the period 1973 to 2001(especially the previous government ‘derg’ regime) there was a reforestation and afforestation programmes to preserve indigenous trees or forests and planting of trees. Generally, during the 1st and 2nd period of the study 131 Km^2 (24.04% of the forest) and 87 Km^2 (31 % of the forest) respectively was afforested mainly of eucalyptus and conifers type of trees. By an increase of population in the area there is also an increasing need to fire wood. As a consequence also the remaining forested areas became further under pressure and, in general, land cover changes in the

forest area were quite significant. Consequently, the clearing of forest and the increase in agriculture land has resulted to gully erosion in several parts of the catchment as shown in figure 5.7.

Figure 5-7: Gully erosion near Sekela town.

5.5. Hydrological response to land cover change

5.5.1. High flow and low flow analysis

Time series of stream flow for the Upper Gilgel Abbay were analysed for the years 1973−2003 using a statistical method. The method serves to assess to what extent changes in observed stream flow series can be observed. In stream flow frequency analysis most often cumulative distributions and probability of exceedence are used (Nancy, 2004). For this study the statistical significance of high flow and low flow was evaluated using the probability of exceedence. The basic procedure of the analysis begins with a ranking of the most extreme events of the past. The stream flow data was sorted in ascending order and then ranked. Each value was assigned a probability of exceedence, that is, the probability that the given value would be equalled or exceeded in any given year.

Let [Xi] denote the observed values and $X_{(i)}$, the i^{th} largest value in a sample, so that $X_{(n)} \leq X_{(n-1)} \leq \text{----} \leq X_{(1).}$ Where FX refers to the frequency of observed values. The random variable U_i defined as

$$U_i = 1 - FX\,[X_{(i)}] \qquad (5.1)$$

corresponds to the exceedence probability associated with the i^{th} largest observation. Here we analysed 30 years of daily discharge data of Gilgel Abbay river. During this period substantial changes in land cover occurred in the basin as describe in Section (5.1) of land cover analysis.

A 5 % exceedence probability represents a high flow that has been exceeded only 5-percent of all days of the flow record. Conversely, a 95-percent exceedence probability would characterize low-flow conditions in a stream since 95 percent of all daily mean flows in the record are larger than that amount. For this study, a 95% and 5% probability of exceedence was chosen to represent the base flow and peak flow respectively. The results of this procedure are presented in figure 2.1 and 2.2.

Based on the available information on the land cover of the catchment, the stream flow data were analysed based on the results of probability of exceedance for the periods 1973-85 and 1986-2003 corresponding to 1973, 1986 and 2001 land cover maps.

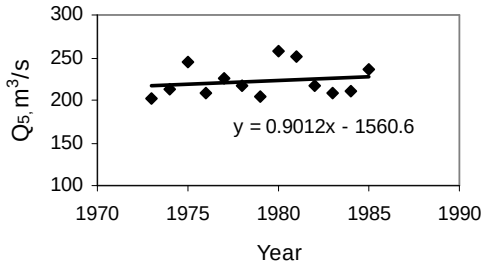

(a) Peak flow

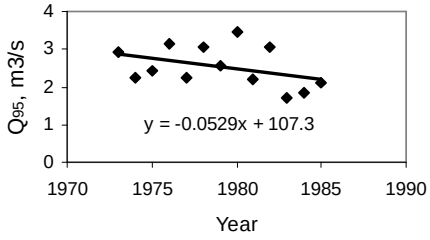

(b) Base flow

Figure 5-8: The 95 % and 5 % exceedence of peak flow and base flows between the years 1973−1985

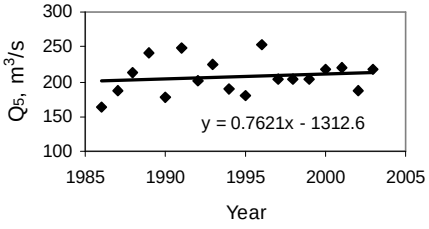

(a) Peak flow

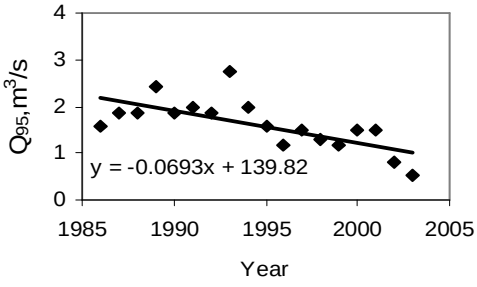

(b) Base flow

Figure 5-9: The 95 % and 5 % exceedence of peak flow and base flow between the years 1986─2003.

As from the 1970s, the linear trend in the high flows in figure 5.8 (Q_5) indicates that the maximum of stream flow increased towards the end of the year 1985 by a rate change of 0.9012 m^3/s. This implied there was a significant change of peak flows during the period of 1973-1985. On the other hand, the trend in the low flow in Q_{95} shows the base flow was highest at the beginning of the selected period but it decreased by a rate of 0.0529 m^3/s for the time period till 1985.

By the objectives of this study it is here hypothesized that the increase in surface runoff and high flows can be explained by the increased area under agriculture. As discussed in section 5.3 and 5.4, agriculture cover has increased by some 12% between 1973 and 1985 at the expense of forest cover. Over the same period and, presumably, as a result of a decreased subsurface flow, the base flow decreased due to less storage of water.

During the second period (1986-2003), high flow analysis shows the stream flow further increased by the rate change of 0.7621m^3/s, where as in the low flow analysis the base flow further decreased by the rate change of 0.0693m^3/s. Similarly, the land cover change during this period was due to increased by the expansion of the agriculture up to 23 % as shown in section 5.2 and 5.3.

5.5.2. Change in seasonal stream flows

In order to analyze the changes in seasonal flows during the period (1973-2003), the wettest months of stream flow are taken as June, July and August; while the driest stream flow are considered in the months of January, February and March. During the wet season, rainfall is at its peak, and a large amount of the stream flow is generated from surface runoff. For the wettest months, flow records for the period 1973-2003, in figure 2.1 show that the stream flow fluctuated between 50-70% of the annual flow. The maximum and the minimum wet season flow recorded 70% in 2002 and 51% in 1978 respectively.

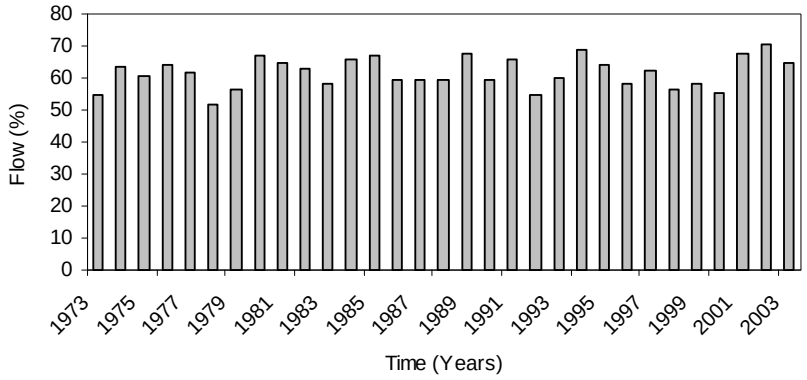

(a) Wet months flow

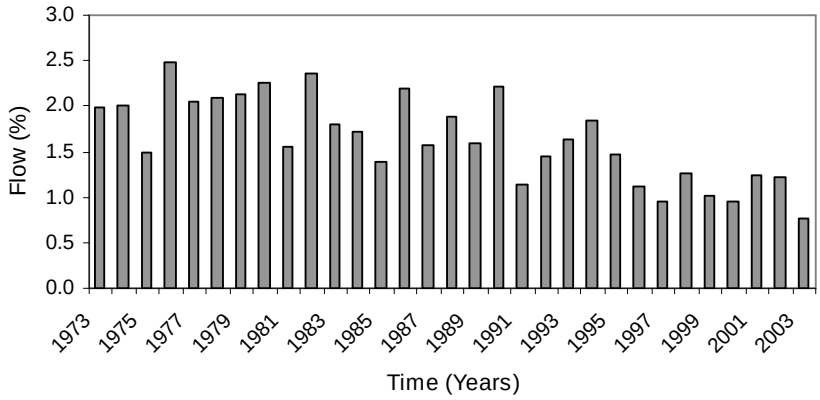

(b) Dry months flow

Figure 5-10: The peak and base flow of Upper Gilgel Abbay river during the period of wet season and dry months (1973-2003).

At it is shown in figure 5.10 the stream flow of the catchment during the dry season fluctuated between 0.5 % - 2.5 % of the annual flow. The maximum and the minimum of dry season flows recorded are 2.5 % in 1977 and 0.8 % in 2003 respectively. In other word, the amount of stream flow during the dry season indicates that it decreased from year to year, on the contrary the flows during the wet season increased.

In relation to stream flow analysis, the analysis of land cover change at section 5.1 indicated that the expansion of agriculture in the catchment during the selected period (1973−2001) changed a decrease of forest by 67.13%.

Empirical Studies have been conducted in different parts of the world to evaluate the effects of changes in land cover on stream flow patterns. Study on a large river basin like Mara river, in Kenya, Mutie (2005) introduced that due to decrease of forest cover and increase of agricultural and pasture lands, the mean peak flow of the river increased as well as the period of the river flows at minimum flow has increased during the dry season over the years. According to Mumeka (1986) deforestation and subsistence of agriculture have a significant increased the amount of runoff from the catchments after the change in the land cover. In their study in an upland watershed in Srilanka, Elkaduwa and Sakthivadievel (1999) discovered that increased surface runoff generation and decreased base flow was mainly caused by reduced infiltration when natural forest cover is converted to other land cover like croplands. The crop land is not as effective as maintaining high infiltration rates. A modelling study of hare watershed, Southern Ethiopia, Tadele (2007) reported that there was an increased river flow for dry season and a decreased river flows for wet season due to the replacement of natural forest into farmland and settlements. In their recent study in the chemoga watershed, in Blue Nile basin, Bewket and Sterk (2005) observed that large volume of surface runoff occurs during the storm events since the area under forest cover decreased.

On the other hand, the change detection approach in section 4.1 shows that there was an afforestation programme on different land cover of the catchment in order to preserve further change on the forest, and that mainly by eucalyptus plantation trees. Many researches done in upper Blue Nile area reported that the observed increased in the afforested area did not improve the hydrological balance in watershed because most of the eucalyptus trees planted are known to absorb a great amount of water. According to Maidment (1993), eucalyptus and pine types cause an average change of 40mm in annual flow for a 10% change in cover, with respect to grasslands in a correlation of inverse proportion. This means that a 10% increase in tree cover causes a decrease of annual flow by 40mm and vice versa.

Generally, hydrological investigation with respect to land cover change within upper Gilgel Abbay catchment showed that the river flow regimes have changed, with increases in peaks and reduction in base flows throughout the selected period of study.

5.6. Hydrological modelling

5.6.1. Model calibration and validation

Calibrated parameters were adjusted manually to match the observed and simulated discharges. It has been check that the calibrated parameter values are within the acceptable ranges as specified in the HBV manual. The optimal calibration parameters obtained are presented in table 5-6.

Table 5-6: The calibrated parameter set of the Upper Gilgel Abbay

Parameters	Description	Range	value
α	Measure of non-linearity to upper response of reservoir	0.5 –1.1	1.1
β	Exponent in equation for discharge from zone of soil water.	1 – 4	2.3
FC	Maximum soil moisture storage (mm)	100 – 1500	120
KHQ	Recession coefficient for upper response box	0.005 – 0.2	0.2
K4	Recession coefficient for lower response box	0.001 – 0.1	0.1
LP	Limit for potential evaporation	<=1.0	0.85
PERC	Percolation from upper to lower response box (mm)	0.01 – 6.0	0.5

Figure 5-11 shows that the shape of observed and the simulated hydrograph have a good agreement in terms of base flow, rising and recession limb, and the peak flows. However, some peaks which occurred mainly at the end of the wet season are underestimated. Most likely under estimation of peak flows caused by 75 % of rain gauge stations are found outside or around the catchment area and this might not represent well the areal pattern of the rainfall over the catchment.

The performance of the HBV model was objectively evaluated by two selected objective function which are the Nash and Sutcliffe efficiency and the relative volume error. The two objective function values are 0.80 and -2.13 % respectively, that suggests a satisfactorily model performance during the calibration period (2000-2003).

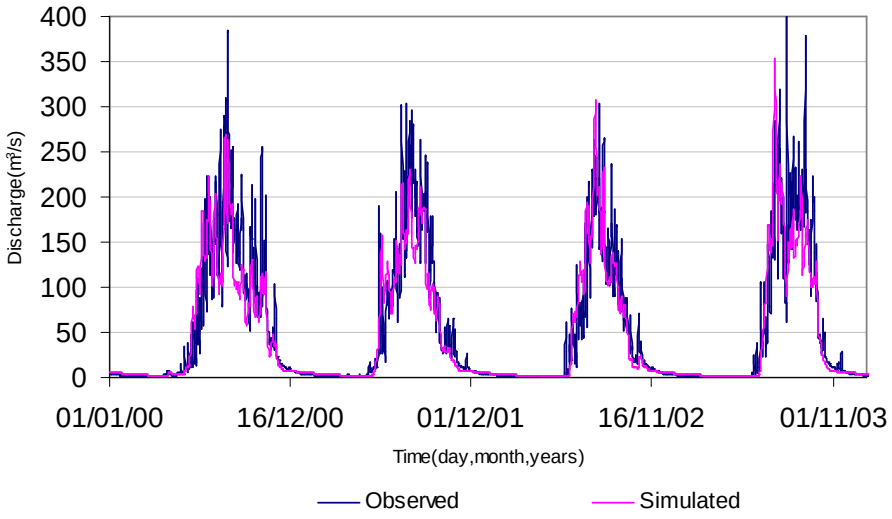

Figure 5-11: The daily observed and simulated hydrograph of the Upper Gilgel Abbey during calibration period

The calibrated parameters were validated through an independent set of flow data during the period of 2004 – 2005. The overall efficiency of the model that is evaluated by Nash and Sutclife (R^2) and the relative volume error (RVE) was 0.77 and 4.72 %, respectively during the validation period. These values reveal that the model results are satisfactory for this study.

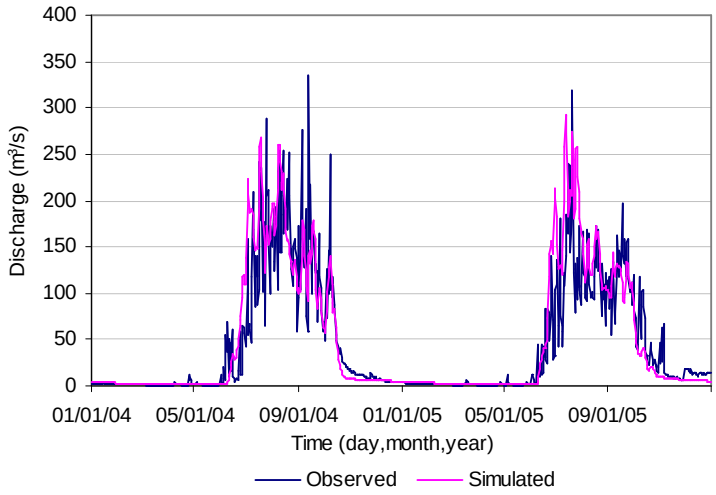

Figure 5-12: The daily observed and simulated hydrograph of the Upper Gilgel Abbay during validation period

This is Body text style. Use this for the body text

5.6.2. Model response to land cover

The daily flow hydrographs that is simulated for the three time periods corresponding to the land cover of 1973, 1986 and 2001 are shown in Figure 5-13. The 2000 – 2003 meteorological forcing served as an input to the HBV model. This allows studying the effect of land cover on the model response which is not affected by changes in the meteorological forcing.

Visual comparison is performed between the hydrographs of the three land cover periods and comparison is based on the peak flow, recession limbs and base flows of the hydrograph. The hydrograph of the year 2002 is considered as reference for comparison.

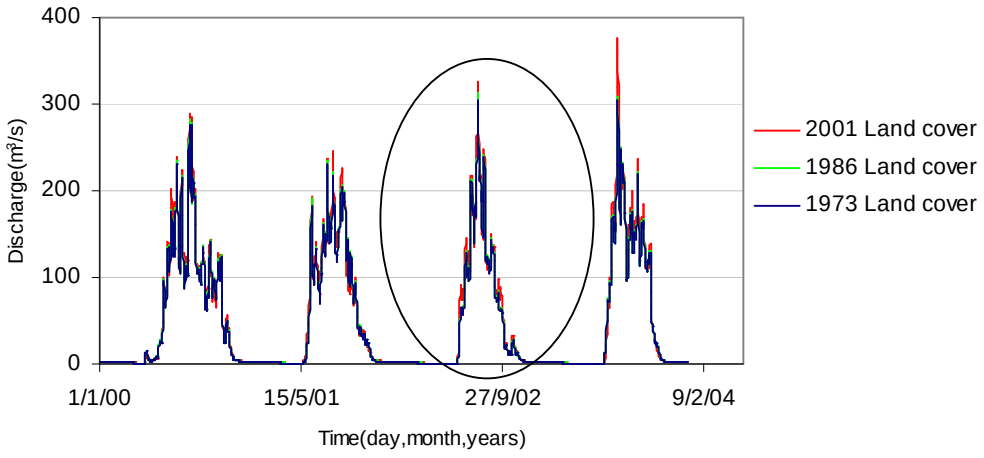

Figure 5-13: Simulated hydrograph for different time periods of land cover

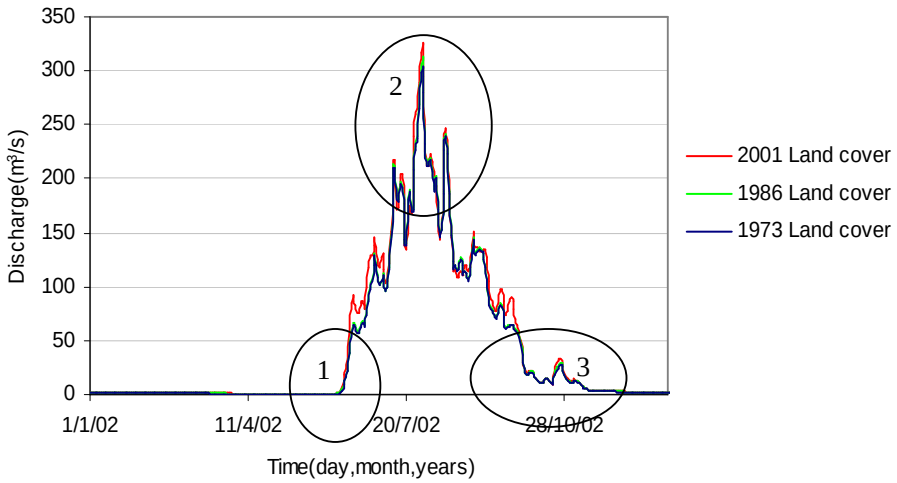

Figure 5-14: Simulated hydrograph selected for one year from the above hydrographs.

In this case the starting of peak flows, peak flows and the recession limb in figure 5-14 are shown by circle 1, circle 2 and circle 3, respectively. Detailed description of each part of the hydrograph is given in the following paragraphs.

Starting of wet season:

The hydrograph at the start of the wet season, which is in June, is shown in figure 5-15. The figure indicated that, for the same meteorological forcing, the flow for the 2001 land cover was infiltrated earliest and the steepest rising limb relative to the flow of the 1986 and 1973 land cover. The land cover of forest during the period of 2001 decreased by 70 % than the 1973 which suggested that deforestation causes the wet-season simulated flow to start early. The 1986 land cover hydrograph also started earlier than the 1973 land cover hydrograph.

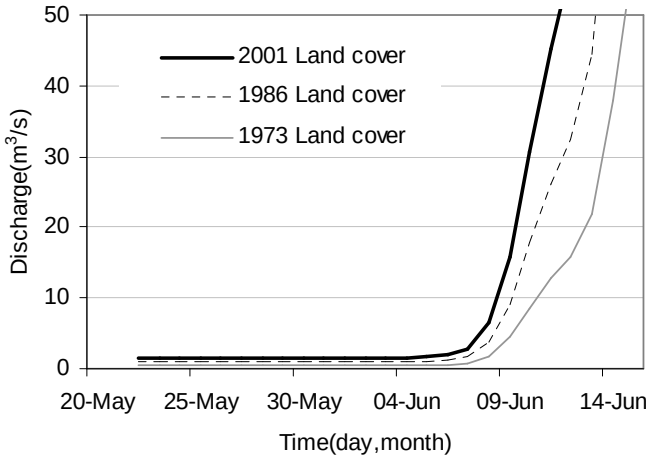

Figure 5-15: The starting of pick flows due to different period of land cover

Peak flows:

Figure 5-16 indicated that peak flows, which occur in July and August, rise earlier with steepest slope and highest peak for the 2001 land cover to that of the 1973 and 1986 land covers. The 1986 land cover also produced somewhat higher peak flow than the 1973 land cover. For the 2001 land cover, much of the rainfall was converted to direct runoff which caused maximum peak flow. On the contrary, the hydrograph of 1973 land cover shows the lowest peak flow since much of the rainfall was lost due to evapotranspiration. Since the largest forested area (51 %) of the 1973 land cover, it generated the highest simulated evapotranspiration during the wet season while the 2001 land cover figure generated the lowest with respect to its forest cover (17%) as shown in figure 5-17.

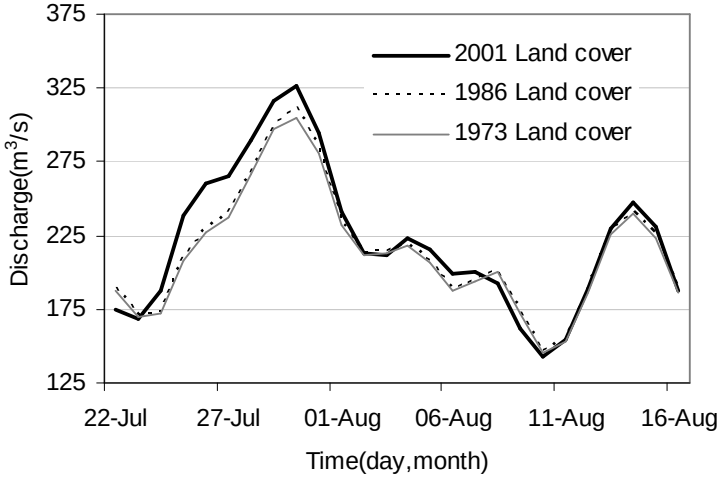

Figure 5-16: Peak flows due to different period of land cover

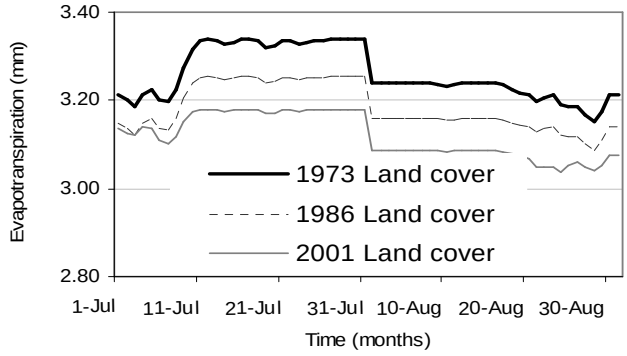

Figure 5-17: Simulated hydrographs of evapotranspiration for the different period of land covers

Recession of flows:

As shown in figure 5-18, the recession of the hydrograph starts at the beginning of October. The simulated hydrograph indicated that, although the difference is small, flows due to the 2001 land cover receding slowly relative to that of the 1986 and 1973 land cover. This implies much of the water was converted to a runoff rather than infiltrate in to base flows or evaporate. Since large area of the

1973 land cover of the catchment was covered by forests, much of the rainfall evaporates relatively to 1986 and 2001 land cover. More over, due to the largest coverage of forest for 1973 land cover, the flow of water become retarded and it will recede rapidly.

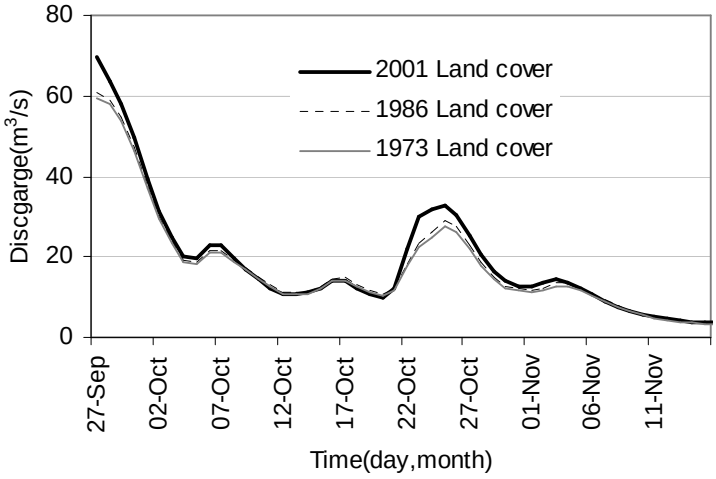

Figure 5-18: Recession limbs due to different period of land cover

Quantitatively, the model response to the land cover was evaluated by comparing the annual, and selected wettest and driest months' flows. The result indicated that the mean annual flow for 2001 land cover was increased by 6.06 % than 1973 land cover. Similarly, the 1986 land cover mean annual flow was higher by 2.48% than the 1973 land cover flow. Figure 17 indicates that June, July and August was selected as wet months flow for different period of land cover. For the three months, the highest flow is simulated for the 2001 land cover. For instance, the wet season, the simulated peak flow for the 2001 land cover is increased by 5.27 % relative to the simulated flow of the 1973 land cover. The simulated actual eavpotranspiration for the 2001 land cover has decreased by 4.31 % relative to that of the 1973 land cover as shown in figure 5.19. In their modelling study of Ketar basin, south central Ethiopia, Legesse et al. (2003) reported that the conversion of forest to agriculture land cover resulted in increased runoff. Generally, flow of the wettest months has increased with the decrease in the forest cover of the catchment.

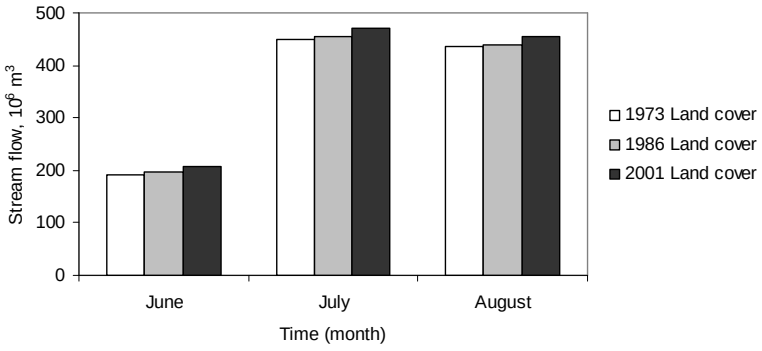

Figure 5-19: The wettest season simulated flow for different periods of land cover

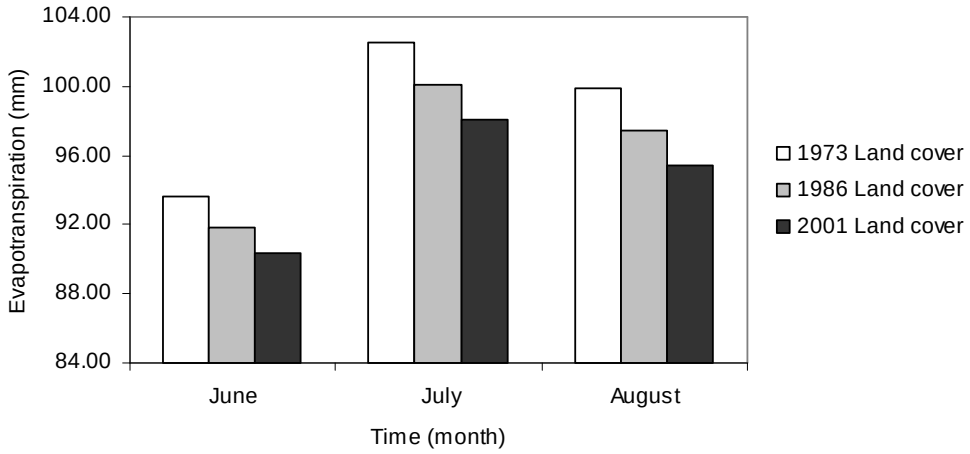

Figure 5-20: The wettest season simulated evapotranspiration for different periods of land cover.

For the flows of the driest season that are January, February and March months are shown in figure 5.22. The figure shows that the lowest base flow occurs in March. The base flow for the 2001 land cover was highest relative to the base flow for the 1986 and 1973 land cover. It was increased by 2.74 % relative to that of the 1973 land cover. The model result in response to land cover change during the dry season is in contrast to the real situation in the catchment. The seasonal flow analysis (see section 5.2) based on the observed time series flow data indicated that the stream flow was decreased as a result of decreased contribution from the base flow during the study period of dry season corresponding to land cover changes (1973-2003).

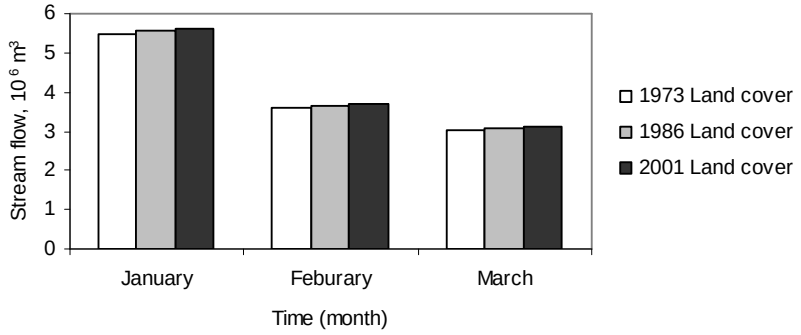

Figure 5-21: The driest season flow for different period of land covers

5.6.3. Impact of land cover change scenario on stream flows

In order to investigate the sensitivity of the hydrological response of the catchment to the changes in the land cover in upper Gilgel Abbay river, two hypothetical land cover scenarios were established and the model was rerun using the same meteorological input used in the calibration and validation periods. The first scenario was generated by changing the whole catchment land cover into field to investigate the impact of deforestation (100 % removal of all forest) on the runoff generation. The

second scenario was used to investigate the effect of dense forest on the hydrology response of the catchment, and it was generated by changing the whole catchment in to a forest land cover.

Based on the two scenarios, the impact of forest cover change on mean annual, wet season and dry season flow was analysed using HBV model under the same meteorological and climatic series over the period of 2000-2003. For instance, the period of year 2002 model is shown in figure 5.23 to illustrate the model response to the effect of two extreme scenarios of land cover change.

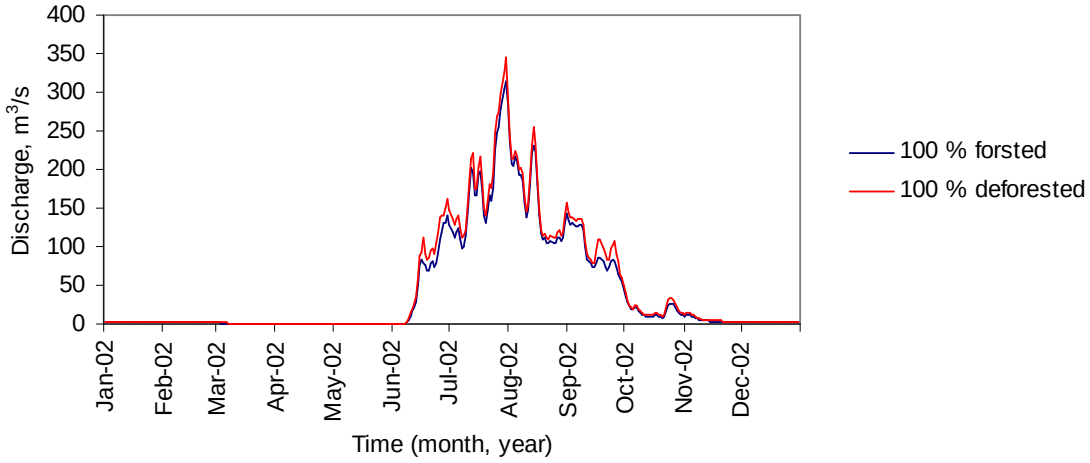

Figure 5-22: simulated hydrograph (2002) for different time period of land cover scenario

The analysis indicted that the 1st scenario, a completely removal of forest at the expense of agriculture land cover, the peak flow increased by 5.82 % during the wet season (see figure 5.24) to that of the second scenario, the whole catchment covered by forest.

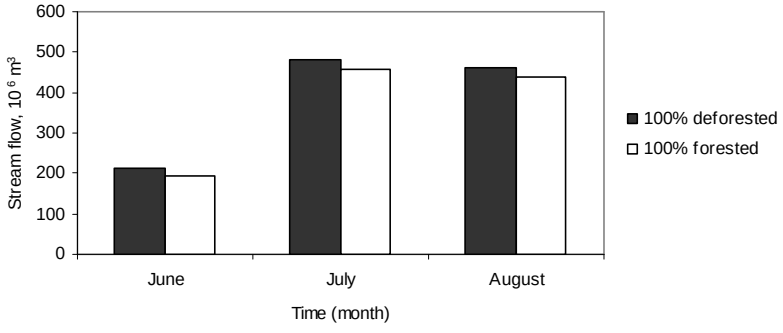

Figure 5-23: Effect of forest cover change scenario during wet season

Similarly, the result showed that 100 % deforestation increased the mean annual flow rate in the entire simulated period of the model increased by 6.53 % as shown in figure 5.23.

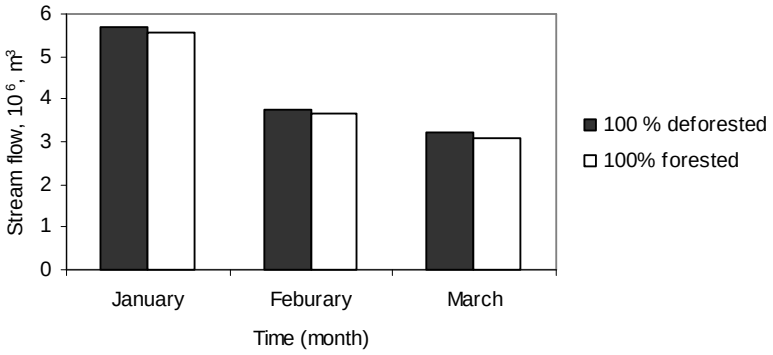

Figure 5-24: Effect of forest coverage scenario during dry season

On the other hand, the model simulated the base flows increased by 3.12 % during dry season (see figure 5.25) for completely deforested land cover of the catchment to that of fully covered by forest land.

In general, in this study to investigate the response of the hydrologic model to the forest cover changes scenario during the dry season is likely unrealistic. In accordance with the presented time series observed flow data analysis (see section 5.2) confirmed that the base flow of the catchment was decreased corresponding to the forest reduced during the whole

6. CONCLUSIONS AND RECOMMENDATIONS

6.1. Conclusion

In this study, satellite data and GIS were integrated with a hydrological model to evaluate the impacts of land cover change in the upper Gilgel Abbey river of Lake Tana basin. Use of GIs and remotely sensed data were found to be helpful tools to detect and analyse spatiotemporal land cover dynamics. These techniques were applied to enable and asses of the land cover dynamic effects on the hydrology of the basin. The impacts of land cover change on stream flow was analysed both statistically and using the hydrological model, HBV. Based on the results obtained and their analyses, the following conclusions are drawn:

- The analysis of the land cover classification and change detection using integrated remote sensing data and GIS technique over a period of years both in a spatially, quantitative way in Upper Gilgel Abbay catchment revealed that there was a significant and continuous change in forest area as caused by (most prominently) increase of agriculture activity in the catchment. The result of the analysis was inferred that forest cover of 51 % in the catchment decreased to 17 % and the expansion of agricultural land from 28 % to 62% during the study period of 1973−2001.

- Changing in river flow was analysed using the observed time series hydrological data correspond to the land cover change period. The result showed that an increasing trend of the peak flow by a rate change of 0.9012 m^3/s and 0.7621 m^3/s during the period of 1973-1985 and 1986-2003 respectively, and a decreasing trend of the base flow by the rate change of 0.0529 m^3/s and 0.0693 m^3/s with respect to the their study period. Hence, a lot of measures should be taken to sustain the water resource and to maintain a balanced dry season stream flow aimed at reducing the magnitudes of surface runoff generation and increasing ground water recharge in the watershed.

- The hydrological modelling result showed that the HBV model simulated the runoff satisfactorily. Performance of the model for both the calibration and validation catchment were found to be reasonably good with Nash-Sutcliffe coefficients (R^2) value 0.80 and 0.77 for the calibration and validation respectively.

- The result of model for different period of land cover (1973, 1986 and 2001) indicated that the mean annual flow for 2001 land cover was increased by 6.06 % relative to that of 1973 land cover period while the peak flow for 2001 land cover was also increased by 5.27 % than the 1973 land cover. On the contrary, the base flow for 2001 land cover was increased by 2.01 % than the 1973 land cover. Similarly, the result of model response for the land cover scenario confirms that the annual flow and peak flow for completely deforested of the catchment was increased by 6.53 % and 5.82 % respectively relative to that of 100 % forested. The result of model response also showed that the base flow for completely removed

forest was increased by 2.75 % relative to that of forested the whole catchment. The base flow results are contradicted our hypothetical and the realistic situation of the catchment.

6.2. Recommendation

In view of the conclusions, the following suggestions are made:

- For future detailed study of the land cover in the catchment the overall accuracy and kappa statistic of the classified image can be increased by taking more ground control points integrated with aerial photos which cover the whole area of the study.

- This study enables to enhance for further study to predict the impact land cover changes on stream flows by developing different scenarios simulation and optimization strategies that provide valuable information to devise more effective watershed management in the area.

- The performance of the model can be improved by increasing the number of rainfall and discharge gauging station with in the catchment. So, for future similar the historical time series land cover studies in the larger river basins like Upper Blue Nile and other areas in country it is recommended to use radar or other satellite rainfall data integrated with the point measurements on the ground.

- Dry season flows are an important component from a management perspective. There fore, further work could be undertaken to asses the effect on the dry season flows of biasing the calibration of the reference catchment towards low flows.

REFERENCE

Allen, R. (1998). Crop Evapotranspiration: Guidelines for computing crop water requirements. FAO, Rome.

Alphan, H. (2003). Land-use change and urbanization of Adana, Turkey. Land Degrad. Dev. 14, 575.

Ashenafi, S. (2007). Catchment modelling and preliminary application of isotopes for model validation in upper Blue Nile Basin, Lake Tana, Ethiopia. UNESCO-IHE.

Bewket, W. (2003). Dynamics in land cover and its effect on stream flow in the chemoga water shed, Blue Nile basin, Ethiopia. Hydro. Processes, Vol. 19, Issue 2, pp. 445-458.

Calder, R. (1995). The impact of land use change on water resources in sub-Saharan Africa: a modelling study of Lake Malawi. J. Hydrol, 170, 123–135.

Calder, I. (2002). Forests and hydrological services: reconciling public and science perceptions. Land Use and Water Resources Research 2, 2.1-2.12 (www.luwrr.com)

Coppin, P. & Bauer, M. 1996. Digital Change Detection in Forest Ecosystems with Remote Sensing Imagery. Remote Sensing Reviews. Vol. 13.p.207-234.

Croke, B.F.W. (2004). A dynamic model for predicting hydrologic response to land covers changes in gauged and ungauged catchments. J. Hydrol, 291, 115–131.

EMA (Ethiopian Meterlogical Agency). 1999. Meterlogical Report of 1981. Addis Abeba, Ethiopia: Ethiopian Meterological Agency.

Flugel, L. A. (1995). Delineating hydrological response units by geographical information system analyses for regional hydrological modelling in the drainage basin. Hydrology WRP, pp.181-109.

Goetz, A.F.H., Mckintosh, P.J., and Leslak, L.R. (1999). Multiyear calibration of Landsat TM for studies of land use and land use change in the high plains. In: Proceedings 13th International Conference Applied Geologic Remote Sensing, 1–3 March 1999. Ann Arbor, MI: ERIM, II, p. 183.

Herold, M. (2003). The spatiotemporal form of urban growth: Measurement, analysis and modeling. Remote Sens. Environ. 6, 286.

Hashiba, H., Kameda, K., Uesugi, S., and Tanaka, S. (2000). Land use change analysis of Tama River Basin with different spatial resolution sensor data by Landsat/MSS and TM. Adv. Space Res. 26, 1069.

Huete A.R. & C.J. Tucker 1991. Investigation of soil influences in AVHRR red and near- infrared vegetation index imagery. International Journal of Remote Sensing 12, 6: 1223-1242.

Hurni, H. 1993. Land degradation, famine, and land resource scenarios in Ethiopia. In: Pimentel D, editor. World Soil Erosion and Conservation. Cambridge Studies in Applied Ecology and Resource Management. Cambridge, UK: Cambridge University Press, pp 27–61.

Kahsay, B. (2004). Land use and land cover change in central high lands of Ethiopia. MSc research paper, Addis Ababa University.

Legesse, D. (2003). Hydrological response of a catchment to climate and land use changes in tropical Africa: case study South Central Ethiopia. T. Hydrol, 275, 67-85.

Liden, R. (2000). Analysis of conceptual rainfall-runoff modeling performance in Different climates. J.Hydrol, 238:231– 247

Lindstrom, G. (1997). Development and test of the distributed HBV-96 hydrological model.

Maidment, D.R. 1993. Hand book of hydrology, Mc Graw – Hill, New York, pp.113.

Maingi, J.K. (2001). Assessment of environmental impacts of river basin development on the riverine forests of eastern Kenya using multi-temporal satellite data. International Journal of Remote Sensing, 22(14):2701-2729.

Monserud, R. A., 1990: Methods for comparing global vegetation maps. Working Paper WP-90-40, IIASA, Laxenburg, Austria, 22 pp. [Available from International Institute for Applied Systems Analysis, Schlossplatz 1, Laxenburg A-2361, Austria.]

Meyer, W.B. and Turner, B.L. II, editors. 1994. Changes in land use and Land cover: A Global Perspective. Cambridge: Cambridge University Press. 537 p as cited in Meyer, W.B., 1995.

Nancy, D. (2004). Stream hydrology: An introduction for Ecologies, Second Edition. Pp 201-214.

Nash, J.E., Sutcliffe, J.V., 1970. River flow forecasting through conceptual models. Part I: a discussion of principles, J. Hydrol., 10, 282-290.

Parkin, G. (1996). Validation of catchment models for predicting land-use and climate change impacts. 1. Case study for a Mediterranean catchment. J. Hydrol. 175, 595–613.

Prol-Ledesma, R.M., Uribe-Alcantara, E.M., and Diaz-Molina, O. (2002). Use of cartographic data and Landsat TM images to determine land use change in the vicinity of Mexico City. *Int. J. Remote Sens.* 23, 1927.

Refsgaard, J.C. (1996). Terminology, modeling protocol and classification of hydrological models. In: Abbott, M.B., Refsgaard, J.C. (Eds.), Distributed Hydrological Modeling. Kluwer, Dordrecht, pp. 17–39.

Ridd, M.K., Merola A.J., and Jaynes, R.A. (1983). Detecting agricultural to urban land use change from multi-temporal MSS digital data. In: Proceedings of Acsm-Asp Fall Convention 1983, Salt Lake City, Utah, and pp. 473.

Rientjes, T. H. M. (2007). Modelling in Hydrology. ITC Enschede, the Netherlands, p.231

Santhi, C. (2001). Validation of the SWAT Model on a large River Basin with Point and Nonpoint sources, Journal of the American Water Resources Association, Vol. 37, NO. 5, pp. 1169-1188.

Savenije, H.H.G. (1995). New definitions for moisture recycling and the relation with land-use changes in the Sahel. J. Hydrol.167, 57–78.

Scott, H.D. and K.R. Hofer (1995). Spatial and temporal analysis of the morphological and land use characteristics of the Buffalo River watershed, Arkansas Water Resources Center Publication number: MSC_170, University of Arkansas, Fayetteville, Arkansas.

Seibert, J. (2002). HBV light: version 2 user's manual. Department of Earth Sciences, Hydrology, Uppsala University, Sweden.

Singh, A. (1989). Digital change detection techniques using remotely sensed data. Int. J. Remote Sens. 10, 989.

Stefanov, W.L. (2001). Monitoring urban land cover change: An expert system approach to land cover classification of semiarid to arid urban centers.

Sunar, F. (1998). Analysis of changes in multidate data set: a case study in Ikitelli area, Istanbul, Turkey. Int. J. Remote Sensing 19, 225.

Tekle, K. and Hedlund, L., 2000. Land changes between 1958 and 1986 I Kalu District, Southern Wello, Ethiopia. Mountain Research and Development Vol20, No 1, pp 42-51.

Tessema, S.M. (2006). Assessment of temporal hydrological variations due to land use changes using remote sensing/GIS: a case study of Lake Tana Basin, Master Thesis, KTH, Sweden.

Tracy J. Baldyga, 2007. Assessing land cover change in Kenya's Mau Forest region using remotely sensed data. African J. Ecol, volume 46 issue pp. 46-54.

Xiao, J. (2005). Evaluating urban expansion and land use change in Shijiazhuang, China, by using GIS and Remote Sensing. Landscape Urban Plan .75.

Wilson, E.H. (2003). Development of a geospatial model to quantify, describe and map urban growth. Remote Sens. Environ. 275.

ANNEX

A- **Elevation and Vegetation Zone of the catchment**

Land cover zone and area coverage of the catchment in each subbasin by 100 m elevation difference.

For the period of 2001 land cover

Subbasin 1

No	Average Elevation m	Land cover	Area (Km^2)	%
1	1975	Field	1.10	0.46
2	1975	Forest	0.72	0.30
3	2075	Field	15.03	6.27
4	2075	Forest	3.57	1.49
5	2175	Field	19.02	7.93
6	2175	Forest	7.57	3.15
7	2375	Field	19.47	8.12
8	2375	Forest	11.11	4.63
9	2275	Field	20.34	8.48
10	2275	Forest	9.58	3.99
11	2475	Field	21.64	9.02
12	2475	Forest	10.25	4.27
13	2575	Field	24.19	10.08
14	2575	Forest	8.93	3.72
15	2675	Field	18.29	7.62
16	2675	Forest	6.84	2.85
17	2775	Field	13.04	5.43
18	2775	Forest	4.79	2.00
19	2875	Field	7.65	3.19
20	2875	Forest	2.53	1.05
21	2975	Field	3.86	1.61
22	2975	Forest	1.52	0.63
23	3075	Field	1.73	0.72
24	3075	Forest	0.79	0.33
25	3175	Field	1.32	0.55
26	3175	Forest	0.52	0.22
27	3375	Field	1.56	0.65
28	3375	Forest	0.21	0.09
29	3275	Field	1.51	0.63
30	3275	Forest	0.42	0.18
31	3475	Field	0.77	0.32
32	3475	Forest	0.07	0.03

Subbasin 2

No	Average Elevation m	Land cover	Area (Km^2)	%
1	1975	Field	57.77	23.46
2	1975	Forest	8.48	3.44
3	1909.5	Field	1.75	0.71
4	1909.5	Forest	0.26	0.11
5	2075	Field	98.93	40.17
6	2075	Forest	9.69	3.93
7	2175	Field	25.98	10.55
8	2175	Forest	5.45	2.21
9	2275	Field	12.93	5.25
10	2275	Forest	3.56	1.45
11	2375	Field	10.14	4.12
12	2375	Forest	2.81	1.14
13	2475	Field	3.39	1.37
14	2475	Forest	1.85	0.75
15	2575	Field	1.91	0.78
16	2575	Forest	0.87	0.35
17	2675	Field	0.27	0.11
18	2675	Forest	0.19	0.08
19	2775	Field	0.04	0.02

Subbasin 3

No	Average Elevation m	Land cover	Area (Km^2)	%
1	1975	Field	18.9054	5.08
2	1975	Forest	1.863	0.50
3	2075	Field	41.0265	11.03
4	2075	Forest	4.9653	1.33
5	2175	Field	56.7162	15.24
6	2175	Forest	8.91	2.39
7	2275	Field	42.7113	11.48
8	2275	Forest	8.5779	2.31
9	2375	Field	89.1162	23.95
10	2375	Forest	6.6825	1.80
11	2475	Field	30.7881	8.27
12	2475	Forest	4.6413	1.25
13	2575	Field	32.724	8.79
14	2575	Forest	4.8762	1.31
15	2675	Field	12.8385	3.45
16	2675	Forest	2.997	0.81
17	2775	Field	1.944	0.52
18	2775	Forest	1.296	0.35
19	2875	Field	0.0243	0.01
20	2875	Forest	0.486	0.13

Subbasin 4

No	Average Elevation m	Land cover	Area (Km^2)	%
1	2175	Field	70.6725	12.49
2	2175	Forest	11.4129	2.02
3	2075	Field	25.9362	4.58
4	2075	Forest	11.6478	2.06
5	2275	Field	90.7929	16.05
6	2275	Forest	17.3583	3.07
7	2375	Field	64.7028	11.44
8	2375	Forest	17.6904	3.13
9	2475	Field	65.1645	11.52
10	2475	Forest	15.8841	2.81
11	2575	Field	70.9803	12.55
12	2575	Forest	15.3981	2.72
13	2675	Field	47.0853	8.32
14	2675	Forest	11.4615	2.03
15	2775	Field	15.5844	2.75
16	2775	Forest	5.8563	1.04
17	2875	Field	4.8519	0.86
18	2875	Forest	1.7253	0.30
19	2975	Field	1.1178	0.20
20	2975	Forest	0.2673	0.05
21	3075	Field	0.1053	0.02
22	3075	Forest	0.0081	0.00

Subbasin 5

No	Average Elevation m	Land cover	Area (Km^2)	%
1	1975	Field	99.70	42.96
2	1975	Forest	10.88	4.69
3	1909.5	Field	5.43	2.34
4	1909.5	Forest	1.04	0.45
5	2075	Field	91.68	39.50
6	2075	Forest	8.55	3.68
7	2175	Field	13.73	5.92
8	2175	Forest	1.09	0.47

For the period of 1986 land cover

Subbasin 1

No	Average Elevation, m	Land cover	Area (Km^2)
1	1975	Forest	0.42
2	1975	Field	1.40
3	2075	Forest	4.60
4	2075	Field	14.00
5	2175	Forest	13.96
6	2175	Field	12.62
7	2375	Forest	16.85
8	2375	Field	13.74
9	2275	Forest	16.28
10	2275	Field	13.64
11	2475	Forest	15.43
12	2475	Field	16.46
13	2575	Forest	14.15
14	2575	Field	18.63
15	2675	Forest	10.23
16	2675	Field	14.17
17	2775	Forest	6.88
18	2775	Field	10.51
19	2875	Forest	3.47
20	2875	Field	6.59
21	2975	Forest	2.07
22	2975	Field	3.16
23	3075	Forest	1.18
24	3075	Field	1.30
25	3175	Forest	0.88
26	3175	Field	0.96
27	3375	Forest	0.66
28	3375	Field	1.12
29	3275	Forest	0.84
30	3275	Field	1.09
31	3475	Forest	0.27
32	3475	Field	0.52

Subbasin 2

No	Average Elevation, m	Land cover	Area (Km^2)
1	1975	Forest	13.24
2	1975	Field	53.01
3	1909.5	Forest	0.60
4	1909.5	Field	1.40
5	2075	Forest	14.50
6	2075	Field	94.11
7	2175	Forest	9.91
8	2175	Field	21.52
9	2275	Forest	7.29
10	2275	Field	9.20
11	2375	Forest	5.97
12	2375	Field	6.98
13	2475	Forest	3.55
14	2475	Field	1.68
15	2575	Forest	1.52
16	2575	Field	1.26
17	2675	Forest	0.24
18	2675	Field	0.21
19	2775	Forest	0.02
20	2775	Field	0.02

Subbasin 3

No	Average Elevation, m	Land cover	Area (Km^2)
1	1975	Forest	4.4307
2	1975	Field	16.3377
3	2075	Forest	9.2907
4	2075	Field	36.7011
5	2175	Forest	18.1035
6	2175	Field	46.656
7	2275	Forest	16.8561
8	2275	Field	34.2711
9	2375	Forest	24.3405
10	2375	Field	70.7778
11	2475	Forest	10.4814
12	2475	Field	23.5872
13	2575	Forest	13.2354
14	2575	Field	23.8059
15	2675	Forest	6.2127
16	2675	Field	8.4726
17	2775	Forest	1.5552
18	2775	Field	1.215
19	2875	Forest	0.0729
20	2875	Field	0.0405

Subbasin 4

No	Average Elevation, m	Land cover	Area (Km^2)
1	2175	Forest	26.8434
2	2175	Field	55.242
3	2075	Forest	9.9144
4	2075	Field	27.6696
5	2275	Forest	47.7252
6	2275	Field	60.426
7	2375	Forest	41.3829
8	2375	Field	41.0103
9	2475	Forest	36.3852
10	2475	Field	44.6634
11	2575	Forest	32.643
12	2575	Field	52.407
13	2675	Forest	21.9591
14	2675	Field	34.4088
15	2775	Forest	8.7723
16	2775	Field	10.9593
17	2875	Forest	2.6649
18	2875	Field	2.8512
19	2975	Forest	0.3888
20	2975	Field	0.486
21	3075	Forest	0.0567
22	3075	Field	0.0567

Subbasin 5

No	Average Elevation, m	Land cover	Area (Km^2)
1	1975	Forest	22.9878
2	1975	Field	87.5934
3	1909.5	Forest	1.3527
4	1909.5	Field	5.1192
5	2075	Forest	18.3546
6	2075	Field	80.7489
7	2175	Forest	2.1384
8	2175	Field	12.6846

For the period of 1973 land cover

Subbasin 1

No	Average Elevation, m	Land cover	Area (Km^2)
1	1975	Field	1.37
2	1975	Forest	0.45
3	2075	Field	8.16
4	2075	Forest	10.45
5	2175	Field	5.60
6	2175	Forest	20.99
7	2275	Field	5.85
8	2275	Forest	24.07
9	2375	Field	22.48
10	2475	Forest	20.70
11	2375	Field	8.11
12	2475	Forest	11.19
13	2575	Field	19.11
14	2575	Forest	13.62
15	2675	Field	12.70
16	2675	Forest	11.57
17	2775	Field	8.42
18	2775	Forest	8.93
19	2875	Field	4.52
20	2875	Forest	5.52
21	2975	Field	2.52
22	2975	Forest	2.71
23	3075	Field	1.49
24	3075	Forest	1.00
25	3175	Field	1.24
26	3175	Forest	0.60
27	3375	Field	0.69
28	3375	Forest	1.09
29	3275	Field	1.38
30	3475	Forest	0.38
31	3475	Field	0.41
32	3375	Forest	0.55

Subbasin 2

No	Average Elevation, m	Land cover	Area (Km^2)
1	1975	Field	34.4088
2	1975	Forest	31.8411
3	1909.5	Field	0.5832
4	1909.5	Forest	1.4256
5	2075	Field	62.2809
6	2075	Forest	46.332
7	2175	Field	14.175
8	2175	Forest	17.2611
9	2275	Field	5.7591
10	2275	Forest	10.7325
11	2375	Forest	8.9424
12	2475	Forest	4.0743
13	2375	Field	4.0095
14	2475	Field	1.1583
15	2575	Forest	2.0007
16	2575	Field	0.7776
17	2675	Forest	0.3078
18	2675	Field	0.1539
19	2775	Field	0.0324
20	2775	Forest	0.0081

Subbasin 3

No	Average Elevation, m	Land cover	Area (Km^2)
1	1975	Field	14.7906
2	1975	Forest	5.9778
3	2075	Field	27.6534
4	2075	Forest	18.3384
5	2175	Field	36.9036
6	2175	Forest	27.8802
7	2275	Field	27.2565
8	2275	Forest	23.8626
9	2375	Forest	28.1961
10	2475	Forest	12.5793
11	2375	Field	66.8331
12	2475	Field	21.4812
13	2575	Forest	14.8554
14	2575	Field	22.1454
15	2675	Forest	7.2981
16	2675	Field	7.3791
17	2775	Field	1.0611
18	2775	Forest	1.7253
19	2875	Forest	0.0648
20	2875	Field	0.0324

Subbasin 4

No	Average Elevation, m	Land cover	Area (Km^2)
1	2075	Field	19.1808
2	2075	Forest	18.4032
3	2175	Field	27.1674
4	2175	Forest	54.918
5	2275	Field	37.2843
6	2275	Forest	70.8669
7	2375	Forest	55.7523
8	2475	Forest	48.4218
9	2375	Field	26.6409
10	2475	Field	32.6268
11	2575	Forest	42.444
12	2575	Field	42.4926
13	2675	Forest	25.5717
14	2675	Field	30.537
15	2775	Field	9.9954
16	2775	Forest	9.558
17	2875	Forest	2.7864
18	2875	Field	2.6649
19	2975	Field	0.4131
20	2975	Forest	0.4536
21	3075	Forest	0.0486
22	3075	Field	0.0648

Subbasin 5

No	Average Elevation, m	Land cover	Area (Km^2)
1	1975	Field	62.5482
2	1975	Forest	48.033
3	1909.5	Field	3.4668
4	1909.5	Forest	3.0051
5	2075	Field	56.4651
6	2075	Forest	42.606
7	2175	Field	7.3629
8	2175	Forest	7.4601

B-General procedure to obtain relevant information from DEM

The procedure to obtain relevant hydrological information from SRTM DEM